Neurobiology of Disease 202 (2024) 106698

Contents lists available at ScienceDirect

Neurobiology of Disease

journal homepage: www.elsevier.com/locate/ynbdi

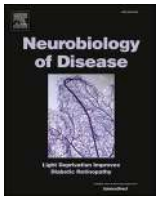

Multiomics approach discloses lipids and metabolites profiles associated to Parkinson's disease stages and applied therapies

Federica Carrillo [a], Nicole Piera Palomba [b], Marco Ghirimoldi [c], Camilla Didò [c], Giorgio Fortunato [a], Shahzaib Khoso [c], Tiziana Giloni [b], Marco Santilli [b], Tommaso Bocci [d], Alberto Priori [d,e], Sara Pietracupa [b,f], Nicola Modugno [b], Elettra Barberis [g,h], Marcello Manfredi [c,g,1], Paola Signorelli [d,i,1], Teresa Esposito [a,b,*,1]

[a] Institute of Genetics and Biophysics "Adriano Buzzati-Traverso", National Research Council, Naples, Italy
[b] IRCCS INM Neuromed, Pozzilli, IS, Italy
[c] Biological Mass Spectrometry Lab, Department of Translational Medicine, University of Piemonte Orientale, Novara, Italy
[d] "Aldo Ravelli" Center for Neurotechnology and Experimental Brain Therapeutics, Department of Health Sciences, University of Milan, Via Antonio di Rudinì 8, 20142 Milan, Italy
[e] Clinical Neurology Unit, "Azienda Socio-Sanitaria Territoriale Santi Paolo e Carlo", Department of Health Sciences, University of Milan, Via Antonio di Rudinì 8, 20142 Milan, Italy
[f] Department of Human Neuroscience, Sapienza University of Rome, Italy
[g] Center for Translational Research on Autoimmune and Allergic Diseases, University of Piemonte Orientale, Novara, Italy
[h] Department of Sciences and Technological Innovation, University of Piemonte Orientale, Alessandria, Italy
[i] Biochemistry Laboratory, IRCCS Policlinico San Donato, Milano Italy

ARTICLE INFO

Keywords:
Parkinson's disease
Multi-omics analysis
Deep brain stimulation (DBS)
Circulating biomarkers
Mass spectrometry

ABSTRACT

Profiling circulating lipids and metabolites in Parkinson's disease (PD) patients could be useful not only to highlight new pathways affected in PD condition but also to identify sensitive and effective biomarkers for early disease detection and potentially effective therapeutic interventions. In this study we adopted an untargeted omics approach in three groups of patients (No L-Dopa, L-Dopa and DBS) to disclose whether long-term levodopa treatment with or without deep brain stimulation (DBS) could reflect a characteristic lipidomic and metabolomic signature at circulating level. Our findings disclosed a wide up regulation of the majority of differentially regulated lipid species that increase with disease progression and severity. We found a relevant modulation of triacylglycerols and acyl-carnitines, together with an altered profile in adiponectin and leptin, that can differentiate the DBS treated group from the others PD patients. We found a highly significant increase of exosyl ceramides (Hex2Cer) and sphingoid bases (SPB) in PD patients mainly in DBS group ($p < 0.0001$), which also resulted in a highly accurate diagnostic performance. At metabolomic level, we found a wide dysregulation of pathways involved in the biosynthesis and metabolism of several amino acids. The most interesting finding was the identification of a specific modulation of L-glutamic acid in the three groups of patients. L-glutamate levels increased slightly in No L-Dopa and highly in L-Dopa patients while decreased in DBS, suggesting that DBS therapy might have a beneficial effect on the glutamatergic cascade. All together, these data provide novel insights into the molecular and metabolic alterations underlying PD therapy and might be relevant for PD prediction, diagnosis and treatment.

1. Introduction

Parkinson's disease (PD) is a neurodegenerative disease characterized by the progressive loss of dopaminergic neurons of the Substantia Nigra pars compacta (SNpc) (Bloem et al., 2021). Motor symptoms appear when more than 50–70 % of nigrostriatal dopaminergic neurons have been lost; thus, prodromal patients remain undiagnosed early. Up to now, there is no treatment that can slow the death of dopaminergic

* Corresponding author.
E-mail address: teresa.esposito@igb.cnr.it (T. Esposito).
[1] co-last Authors

https://doi.org/10.1016/j.nbd.2024.106698
Received 7 August 2024; Received in revised form 26 September 2024; Accepted 8 October 2024
Available online 18 October 2024

neurons and the progression of PD; the main pharmacological treatments (L-Dopa and dopamine agonists) only improve motor symptoms. After an initial positive response to the therapy, L-dopa induces unfavourable motor side effects, such as dyskinesia interspersed with OFF periods (Coelho et al., 2015).

In the current therapeutic landscape for Parkinson's disease, deep brain stimulation (DBS) has emerged as a leading intervention. DBS has shown remarkable efficacy in relieving motor symptoms and improving the quality of life of people with advanced PD (Hartmann et al., 2019). However, in a subgroup of patients, DBS has been observed to cause psychiatric clinical manifestation and cognitive decline (Aybek et al., 2007; Merola et al., 2011). Recent evidence suggests that mutation of glucosylceramidase beta 1 (GBA1), a key enzyme involved in ceramide metabolism, can influence the response to DBS (Angeli et al., 2013; Avenali et al., 2023), indicating that the efficacy of this treatment could be influenced by specific metabolic alterations which include a potential connection between this approach and lipid engagement.

Lipids, metabolites, and proteins reflect the physiological and pathological status of an individual. Profiling these data types could be useful not only to highlight new pathways affected in PD condition but also to identify sensitive and effective markers for early disease detection and potentially effective therapeutic interventions. In fact, it has been suggested that precision medicine applied to PD should be based on biomarker profiles instead of clinical features, which can change rapidly within a few years, and which largely overlap (Espay et al., 2017). Moreover, alterations in lipid metabolism may play a key role in the pathophysiology of PD (Alecu and Bennett, 2019; Fais et al., 2021; Ikenaka et al., 2019). Ectopic or excessive lipids, in particular anionic lipids, are required to initiate protein aggregation, leading to the formation of Lewy bodies (Fanning et al., 2020; Hellstrand et al., 2013), that contain proteins and lipids such as ceramide and glycosylated ceramide (Kurzawa-Akanbi et al., 2021; Shahmoradian et al., 2019). Furthermore, lipid alterations can influence cellular signalling and inflammatory responses, contributing to the progressive deterioration of dopaminergic neurons characteristic of PD (Estes et al., 2021).

Emerging evidence indicated that peripheral alterations including metabolic dysregulations might precede and contribute to neurodegeneration (Shao et al., 2021). Although many studies have been dedicated to the discovery of biomarkers that may assist the diagnosis of PD, no peripheral blood derived biomarkers have been used clinically at present (Le et al., 2008; Li et al., 2018; Yang et al., 2019). Moreover, biomarkers of therapeutics efficacy are required to ameliorate responses and reduce side effects.

In this study we investigated whether long-term levodopa treatment with or without deep brain stimulation could reflect a characteristic lipidomic and metabolomic signature of PD patients at circulating level. The study cohort included three groups of PD patients, and a group of healthy subjects matched for age, sex and body mass index (BMI). The three groups of PD patients included early-stage PD patients in the first 3 years of disease, not receiving L-Dopa treatment (referred as No L-Dopa), middle-advanced-stage PD patients with disease duration range 7–19 years, undergoing L-Dopa treatment (referred as L-Dopa), and advanced-stage PD patients with disease duration range 19–37 years undergoing L-Dopa treatment with DBS (referred as DBS). Finally, the aim of the study was to identify new altered metabolic pathways and potential biomarkers at circulating levels associated with early- and/or advanced-stage PD as well as with PD specific treatments.

2. Materials and methods

2.1. PD cohort population

804 independent and unrelated PD patients (501 males; 300 familiar and 504 sporadic cases) were recruited at the IRCCS Mediterranean Neurological Institute (MNI) in Pozzilli (Gialluisi et al., 2021; Gialluisi et al., 2020; Palomba et al., 2023; Tirozzi et al., 2021). All PD subjects were of European ancestry and were evaluated by neurologists of the Parkinson Study Group, according to published diagnostic criteria (Postuma et al., 2015). The PD cohort was recruited from June 2015 to December 2017, and from June 2021 to December 2022, with a thorough protocol comprising neurological examination and evaluation of non-motor domains. All the PD patients were of European ancestry and information about family history, demographic characteristics, anamnesis, and pharmacological therapy was also collected. The Movement Disorder Society revised version of the Unified Parkinson's Disease Rating Scale Part III (33 items, maximum score 132; hereafter called UPDRS) was used to assess clinical motor symptoms. These included language, facial expressions, tremor, rigidity, agility in movements, stability, gait and bradykinesia. Cognitive abilities were tested through an Italian validated version of the Montreal Cognitive Assessment (MoCA). Cognitive domains assessed include short-term memory (5 points); visuospatial abilities via clock drawing (3 points), and a cube copy task (1 point); executive functioning via an adaptation of Trail Making Test Part B (1 point), phonemic fluency (1 point), and verbal abstraction (2 points); attention, concentration, and working memory via target detection (1 point), serial subtraction (2 points), digits forward and backward (1 point each); language via confrontation naming with low-familiarity animals (3 points), and repetition of complex sentences (2 points); and orientation to time and place (6 points). The total score was given by the sum of these domains, and then divided by the maximum score that could be obtained (30 points). Non-motor symptoms were assessed through an Italian validated version of Non Motor Symptoms Scale (NMS) for Parkinson's disease. This scale tests 9 items, including cardiovascular domain, sleep/fatigue, mood/cognition, perceptual problems/hallucinations, attention/memory, gastrointestinal, urinary, sexual function, and ability to taste or smell. The 804 PD patients additionally with 282 healthy subjects were analysed by Whole Exome Sequencing (Manuscript in preparation).

Among the 804 PD patients, we selected the 15 patients from the cohort who had had a bilateral DBS implant for a comparable time at the time of recruitment. Patients carrying *GBA1* mutations were excluded. To compare the data of an equal number of patients per group, we selected 16 patients in the initial phase of the disease who were not yet being treated with L-dopa and 16 patients who had been being treated with L-dopa for at least 5 years.

Written informed consent was obtained from all participants. The ethical board of the IRCCS Neuromed approved the study protocols: N°9/2015, N°19/2020 and N°4/2023.

2.2. Sample preparation

Blood samples from PD patients and healthy subjects were collected in blood collection tubes (BD Vacutainer, K2E (EDTA) then, after two centrifugations at 1900*g* for 10 min, plasma was aliquoted and stored at −80 °C. Unique anonymized codes have been assigned to the samples for processing and subsequent analysis, maintaining the confidentiality of personal data. The extraction of plasma lipids was carried out with a biphasic method: 30 μL of plasma was introduced into a tube and extracted with 225 μL of cold MeOH containing a combination of deuterated standards (Splash Lipidomix®). The solution was then vortexed for 10 s, and 750 μL of cold MTBE was added and vortexed for 10 s. The tube was then placed in a thermomixer at 4 °C and vortexed for 6 min at 2000 rpm. After that, 188 μL of water was added, and the tube was vortexed for 10 s and then centrifuged for 2 min at 14,000 rpm at 4 °C. Finally, 300 μL of supernatant was collected and evaporated with a SpeedVac. The dried sample was replenished with 50 μL of a 9:1 MeOH/toluene solution containing the internal standard CUDA (12.5 ng/mL).

Metabolites were extracted as reported by (Barberis et al., 2020). Briefly, 500 μL of an ACN/IPA/water (3:3:2) solution, with tridecanoic acid at 1 ppm as internal standard, was added to 12 μL of plasma. After vertexing, the sample was centrifuged at room temperature for 15 min at 14,500 ×g. The supernatant was then dried in a speed-vacuum. The

sample was derivatized with methoximation (20 μL of Methoxamine, 80 °C, 20 min) and underwent sialylation (90 μL of BSTFA, 80 °C, 20 min). After this, 10 μL of hexadecane (IS) were added to the sample before the GCxGC-MS analysis.

2.3. Lipidomic analysis

For lipidomic analysis, reconstituted samples were analysed with a Vanquish UHPLC system (Thermo Scientific, Rodano, Italy) coupled with an Orbitrap Q-Exactive Plus (Thermo Scientific, Rodano, Italy). Lipid separation was performed using a reversed-phase column (Hypersil Gold™ 150 × 2.1 mm, particle size 1.9 μm) maintained at 45 °C with a flow rate of 0.260 mL/min. Mobile phase A for ESI mode positive consisted of 60:40 (*v*/v) acetonitrile/water with ammonium formate (10 mmol) and 0.1 % formic acid, while mobile phase B was 90:10 isopropanol/acetonitrile (v/v) with ammonium formate (10 mmol) and 0.1 % formic acid, while in the negative ESI mode, the organic solvents for both mobile phases were the same as in the positive with the exception of using ammonium acetate (10 mmol) as a mobile phase modifier. The gradient used was as follows: 0–2 min from 30 to 43 % B, 2–2.1 min from 43 to 55 % B, 2.1–12 min from 55 to 65 % B, 12–18 min at 65 % to 85 % B, 18–20 min at 85 % to 100 % B; 100 % B was held for 5 min, and then the column was allowed to equilibrate to 30 % B for another 5 min. The total running time was 30 min. Mass spectrometry analysis was performed in both positive ion (at 3.5 kV) and negative ion (2.8 kV) modes. Data were collected in a data-dependent top 10 scan mode (ddMS2). MS full-scan survey spectra (mass range *m/z* 80–1200) were acquired with a resolution of $R = 70{,}000$ and target AGC of 1×106. MS/MS fragmentation was performed using high energy c-trap dissociation (HCD) with $R = 17{,}500$ resolution and 1×105 AGC target. The step normalized collision energy (NCE) was set to 15, 30 and 45. The injection volume was 3 μL. For accurate mass-based analysis, regular Lockmass and interrun calibrations were used. An exclusion list for background ions was generated by testing the same procedural sample for both positive and negative ESI modes22. Quality control was ensured by analyzing pooled samples before, at the beginning and at the end of the batches; using blanks to check for residual interference; and using internal standards, directly in plasma or cell samples, which include a series of analyte classes at levels appropriate for the plasma (Avanti SPLASH Lipidomix) and an internal standard (CUDA) prior to liquid chromatography-mass spectrometry (LC–MS) analysis.

Raw data acquired from lipidomic untargeted analysis were processed with MSDIAL software (Yokohama City, Kanagawa, Japan), version 4.24. Peaks were detected, MS2 data were deconvoluted, compounds were identified, and peaks were aligned across all samples. For quantification, the peak areas for the different molecular species detected were normalized using the deuterated internal standard for each lipid class. To obtain an estimated concentration expressed in nmol/mL (plasma), the normalized areas were multiplied by the concentration of the internal standard. An in-house library of standards was also used for lipid identification.

2.4. Metabolomic analysis

Metabolomics results were generated with a LECO Pegasus 4D Time-of-Flight Mass Spectrometer (Leco Corp., St. Josef, MI, USA) equipped with a LECO dual stage quad jet thermal modulator. The GC part of the instrument was an Agilent 7890 gas chromatograph (Agilent Technologies, Palo Alto, CA, USA) equipped with a split/splitless injector. The first dimension column was a 30 m Rxi-5Sil (Restek Corp., Bellefonte, PA, USA) MS capillary column with an internal diameter of 0.25 mm and a stationary phase film thickness of 0.25 μm, and the second dimension chromatographic column was a 2 m Rxi-17Sil MS (Restek Corp., Bellefonte, PA, USA) with a diameter of 0.25 mm and a film thickness of 0.25 μm. High-purity helium (99.9999 %) was used as the carrier gas, with a flow rate of 1.4 mL/min. One μL of sample was injected in splitless mode at 250 °C. The temperature programme was as follow: the initial temperature was 100 °C for 2 min, then ramped 20 °C/min up to 330 °C and then held at this value for 2 min. The secondary column was maintained at +5 °C relative to the GC oven temperature of the first. Electron impact ionisation was applied (70 eV). The ion source temperature was set at 250 °C, the mass range was 25 to 550 *m/z* with an extraction frequency of 32 kHz. The acquisition rates were 200 spectra/s and the modulation period for the 2D analysis was 4 s for the entire run. The modulator temperature offset was set at +15 °C relative to the secondary oven temperature, while the transfer line was set at 280 °C.

The chromatograms were acquired in total ion current mode. Peaks with a signal-to-noise (S/N) value lower than 500.0 were rejected. ChromaTOF version 5.31 was used for the raw data processing. Mass spectral assignment was performed by matching with the NIST MS Search 2.3 libraries and the FiehnLib. An in-house library of standards was also used for the small molecules' identification (Barberis et al., 2021).

LECO ChromaTOF software was used for all acquisition control of metabolomics data, raw data processing and Statistical Compare for alignment of all analytes. The exported data were normalized for internal standards and optimized by lowness normalization using quality control samples.

2.5. Integrative multi-omics analysis

To identify the highly correlated features discriminating PD treatments, we performed Data Integration Analysis for Biomarker discovery using Latent cOmponent (DIABLO) (Singh et al., 2019) of lipidomic and metabolomic data of PD patients (No L-Dopa, L-Dopa and DBS) and controls. Dimension reduction was performed with an information gain algorithm to obtain only significant features among each group using proteomic and lipidomic data separately. The DIABLO R software was used to separately analyze each combination, utilizing the (MixOmics) library. The sPLSDA model was employed to determine the correlation between the metabolomic and lipidomic data for each group. The model was constructed using a 10-fold cross-validation approach with 10 repetitions. The model was initially assessed by calculating the area under the curve (AUC) score for each component of the Partial Least Squares Discriminant Analysis (PLSDA) algorithm. This approach was used to determine the discriminatory strength of the features. Following the evaluation of the AUC score, the association between lipidomic and metabolomic features was analysed using a circle correlation plot in the DIABLO package.

2.6. Analysis of circulating markers

Plasma concentration of IL1-β, TNF-α, adiponectin, BDNF, CXCL1, leptin, resistin, adipsin, ghrelin, FABP3, FABP7, GFAP were evaluated using a Luminex platform (Labospace srl. Milan, Italy) for the simultaneous detection of the above reported proteins, as described elsewhere (Liu et al., 2005). Following the preparation process, blood samples were drawn and analysed within 90 min with a Luminex analyzer. Standard curves for each biomarker were generated using the premixed lyophilised standards provided in the kits. Each sample was measured in triplicate and calculated as *pg/ml*.

2.7. Statistical analysis

Clinical and demographic characteristics were described using, as summary statistics, median and the interquartile range (IQR) or absolute and relative frequencies. Comparisons between PD patients and CNT were evaluated using MedCalc statistical software for continuous variables and Chi-Square test for dichotomous variables. Statistical analyses of lipidomic and metabolomic samples were performed with MetaboAnalyst 6.0 (www.metaboanalyst.org). Statistical Analysis [single factor] function was used to build volcano plots, principal component

analysis (PCA), partial least squares-discriminant analysis (PLS-DA) and heatmaps. Pathway and Enrichment analysis functions were performed to integrate pathway enrichment analysis and pathway topology analysis, starting from significant metabolites found in statistics. Graphpad Prism 8 was used for graphical representation and unpaired student *t*-test, as well as one-way ANOVA and multiple t-test were adopted for statistical analysis. To compare lipids, cytokines and metabolite concentrations with PD endophenotypes Pearson's correlation analysis was carried out with Graphpad 8 and *p*-value was corrected with Bonferroni. ROC analysis was performed with Online ROC Curve Calculator (http://www.rad.jhmi.edu/jeng/javarad/roc/JROCFITi.html).

3. Results

3.1. Study design and clinical features of the study cohort

This work utilizes an approach that integrates lipidomic and metabolomic analysis with cytokines profile in plasma samples to investigate the molecular constituents of pathways that may be disrupted in PD patients and that could be modulated by long-term treatments (graphical abstract). To this aim, we categorized the cohort into three groups of patients based on specific pharmacological and clinical characteristics: No L-Dopa ($N = 16$; in the first 3 years of disease, not receiving L-Dopa treatment), L-Dopa (N = 16; disease duration range 7–19 years undergoing L-Dopa treatment), and DBS ($N = 15$; disease duration range 19–37 years undergoing L-Dopa treatment with DBS) (Table 1). Fifteen PD patients carrying a bilateral DBS implant were selected from a large cohort of 804 PD patients. Subsequently, we selected the two groups of No L-Dopa and L-Dopa patients based on availability of demographic and clinical information and recruited with the same clinical and biological protocol in the same time interval (from 2020 to 2022). No L-Dopa patients were treated with Monoamine oxidase inhibitors (MAOIs) (11 out of 16 patients), MAOIs combined with DOPA agonists (3 out of 16), DOPA agonists (1 out of 16) and 1 patient was not taking any medications (Table 1). We also selected a group of healthy subjects (N = 16 and referred to as Controls) matched for sex, age and body mass index (BMI). Age, sex, and clinical features of enrolled subjects are reported in Table 1. Patients of both L-Dopa and DBS groups presented a more severe clinical phenotype compared to untreated patients (No L-Dopa), considering the presence of levodopa induced dyskinesia (LID), motor symptoms (UPDRS score), non-motor symptoms (NMS), and cognitive impairment (Montreal Cognitive Assessment (MoCA) score). An earlier age at onset was observed in DBS patients (41 ± 9) compared to other PD patients (62 ± 2 for untreated and 58 ± 8 for L-Dopa-treated patients) (Table 1). Remarkably, DBS patients, despite having a longer duration of the disease, exhibited a similar clinical phenotype compared to L-Dopa-treated patients, suggesting the effective motor compensation attributed to DBS treatment (Table 1). At genetic level two DBS patients, showing an earlier onset of the disease (<30 years), were carriers of pathogenic mutations in the *PRKN* gene, the first was homozygous for the c.G1358A:p.W453X nonsense mutation and the second was carrier of the heterozygous mutation c.C823T:p.R275W. Considering the young age of onset of the disease of this patient, we cannot exclude the presence of a second mutation, likely deletion or insertion, in PRKN, that the WES analysis does not allow to detect. No mutations in genes known to cause Parkinson's disease were identified in the other selected patients.

3.2. Long-term treatment PD patients revealed a specific alteration of plasma lipidomic profile

Lipidomic analysis performed on plasma of PD patients enabled the detection and quantification of 898 lipid species belonging to 28 lipid classes including: diacylglycerol (DG), triacylglycerol (TG), phosphatidylcholine (PC), ether-linked phosphatidyl-cholines (PC-O), phosphatidylethanolamine (PE), ether-linked phosphatidyl- ethanolamines (PE-O), phosphatidylinositol (PI), phosphatidylserine (PS), lysophosphatidylcholine (LPC), lysophosphatidylethanolamine (LPE), lysophosphatidylinositol (LPI), ether-linked lyso-phosphatidyl-cholines (LPC-O), plasmalogen phosphatidylethanolamine (PE-P), ether-linked lyso-phosphatidyl-ethanolamines (LPE-O), ceramide (Cer), hexosylceramide (HexCer), dihexosylceramide (Hex2Cer), trihexosylceramide (Hex3Cer), sphingomyelin (SM), sphingoid bases (SPB), cholesterol ester (CE), cholesterol (Cho), sterols (ST), acylcarnitines (CAR), free fatty acid (FA),

Table 1
Demographic and clinical characteristics of the study cohort.

Study Cohort	CTR	No L-Dopa	L-Dopa	DBS	p CTR vs No L-dopa	p CTR vs L-dopa	p CTR vs DBS	p No L-dopa vs L-dopa	p No L-dopa vs DBS	p L-dopa vs DBS
n	16	16	16	15	–	–	–	–	–	–
gender (M/F)	11/5	11/5	11/5	10/5	–	–	–	–	–	–
age (years)	70 ± 4	64 ± 6.7	72.6 ± 1.7	69 ± 9	0.004	0.02	0.6	< 0.0001	0.08	0.1
BMI	26 ± 3	25.9 ± 2.6	25 ± 4	29 ± 3.5	0.9	0.4	0.01	0.4	0.008	0.006
age at onset (years)	NA	62 ± 6.5	64.6 ± 4.4	41 ± 9.3	–	–	–	0.1	<0.0001	< 0.0001
years of disease	NA	2 ± 1.5	7.7 ± 3.7	28 ± 9	–	–	–	< 0.0001	< 0.0001	< 0.0001
LED	NA	115 ± 67	484 ± 213	549 ± 211	–	–	–	–	–	0.7
L-Dopa treatment (months)	NA	NA	73.5 ± 39	290 ± 180	–	–	–	–	–	0.0001
Years from DBS implantation	NA	NA	NA	8.8 ± 3.7	–	–	–	–	–	–
LID	0/16	0/16	10/6	13/2	–	–	–	–	–	–
UPDRS	NA	13.3 ± 6.5	29 ± 20.3	37 ± 24.6	–	–	–	0.006	0.0008	0.33
NMS	NA	29 ± 25.6	92.5 ± 67.2	102 ± 38.5	–	–	–	0.001	< 0.0001	0.6
MoCa	NA	28 ± 2	24.7 ± 5.3	21.2 ± 7	–	–	–	0.02	0.0008	0.12

BMI: Body mass index; AAO: age at onset; H&Y: Hoehn and Yahr; UPDRS: Unified Disease Rating Scale; NMS: Non Motor Symptoms score; MoCA: Montreal Cognitive Assessment; LED: levodopa equivalent dosage; LID: Levodopa induced Dyskinesia (presence/absence). The values were represented as mean ± SD. The two-tailed T-test was used to calculate p-value of cohort variables Age, BMI, AAO, Disease duration, H&Y, UPDRS III, NMS and MoCA; to calculate p-value of Dyskinesia Fisher's exact test was used.

acid-hydroxyl fatty acids (FAHFA), N-acyl ethanolamines (NAE), and Saccaro lipid (SL) (Fig. S1). Among these classes, the most abundant were TG, SM, PC, PC-O, DG and CER (Fig. S1 A). The partial least squares discriminant analysis (PLS-DA) as well as Principal Component analysis (PCA) clearly discriminated among the investigated groups (Fig. 1A and Fig. S1B).

When comparing PD patients versus controls, hierarchical heatmaps of the top 50 modulated lipid species evidenced an increased amount of plasma lipids in PD patients (Fig. 1B-D). The variable of importance in projection (VIP) score highlights the key lipid species that significantly contributed to the observed lipidomic profile, indicating that remodelling of TG and DG characterizes DBS treated patients and controls, differentiating them from other PD treated patients (Fig. 1E). Among these, three species of TGs have long chains (higher than 18 carbons) and polyunsaturated FA, whereas the remaining relevant species bear shorter chains, either saturated or monounsaturated. In particular, two species that reach the highest VIP value in DBS group are TG 60:14, bearing an arachidonic acid (omega 6) and two eicosapentaenoic acids (omega 3) and TG 60:15 with three eicosapentaenoic acids. The abundance of these two TGs was significantly increased in DBS patients compared to the other groups (Fig. S2).

Moreover, a high VIP score is associated with cholesterol ester (Cho

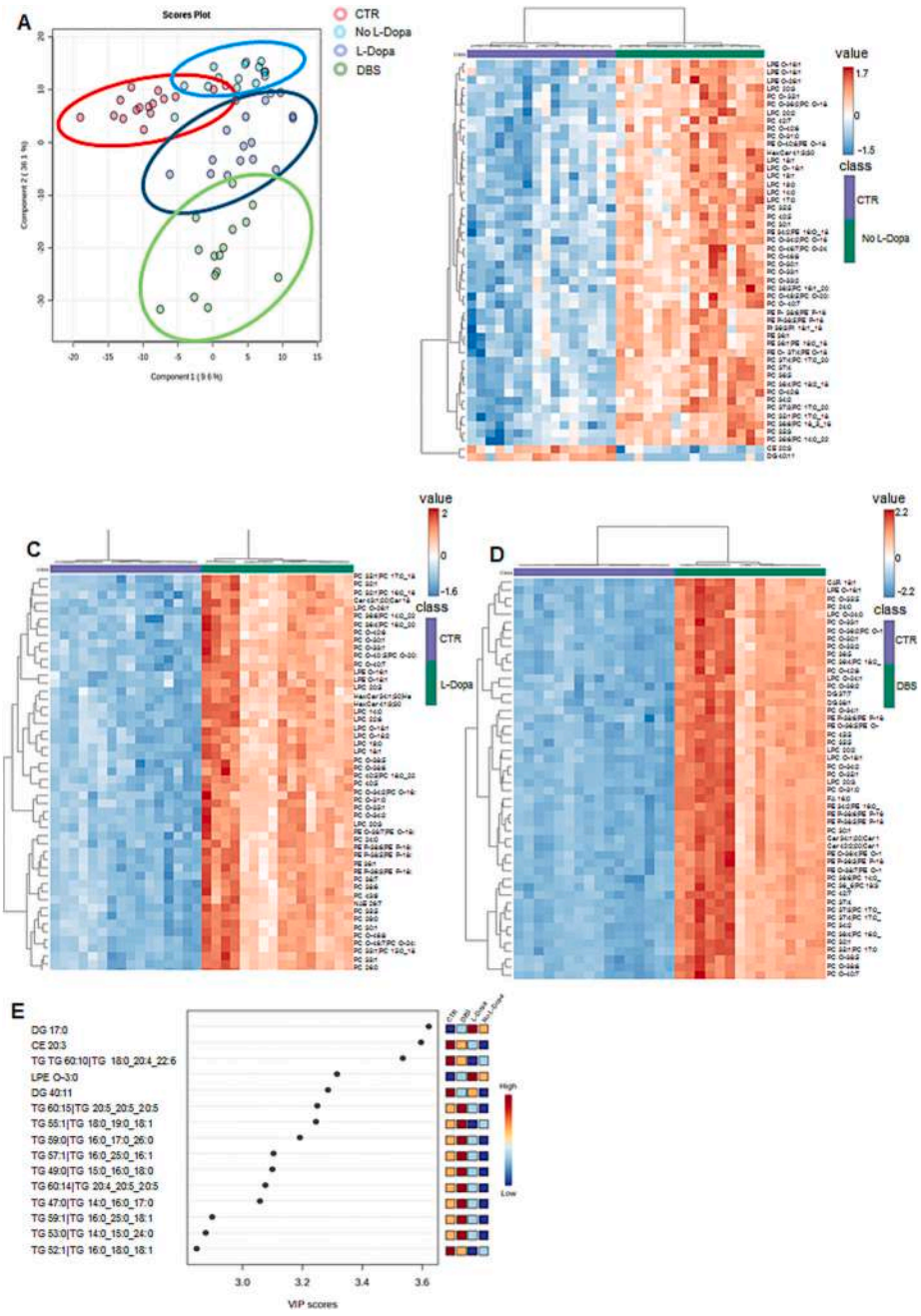

Fig. 1. Heat map representation, supervised PLS-DA and VIP score of plasma lipids. A, Supervised PLS-DA displayed a defined separation of the groups of analysis indicating the percentage of contribution of component 1 and 2 to the variance in the comparison of No L-Dopa, L-Dopa and DBS groups of patients vs healthy subjects (CTR). B—D, Heat map representation of the most 50 differentially expressed lipid species highlighting the clusters of the groups of analysis and an increased amount of lipids in the three PD groups No L-Dopa (B), L-Dopa (C) and DBS (D) compared to healthy subjects (CTR). E, Variable of importance in projection (VIP) scores indicated the most significantly altered lipid species contributing to the different lipidomic profile between No L-Dopa, L-Dopa and DBS groups of patients and healthy subjects (CTR).

C20:3) species that is strongly regulated in DBS (Fig. S2). This Dihomo-γ-linolenic acid (DGLA)- cholesterol is a storage lipid that includes an anti-inflammatory eicosatrienoic acid, which was previously associated with insulin resistance development and cardiovascular disease (Kurotani et al., 2012; Warensjö et al., 2008).

Expression analysis confirmed a significant increase of lipid species in all PD patients (see lipidomic dataset). In particular, we identified 51 downregulated (Fold Change (FC) $\leq$0.7; $p \leq 0.05$) and 357 upregulated (FC $\geq$1.3; $p \leq 0.05$) lipid species when comparing No L-Dopa patients versus healthy subjects (Fig. 2A). 49 downregulated and 460 upregulated lipid species were identified by the contrast L-Dopa versus healthy subjects (Fig. 2A). Finally, 31 downregulated and 450 upregulated lipid species were identified by the contrast DBS versus healthy subjects (Fig. 2A). Next, the FC differences of the species modulated in each lipid

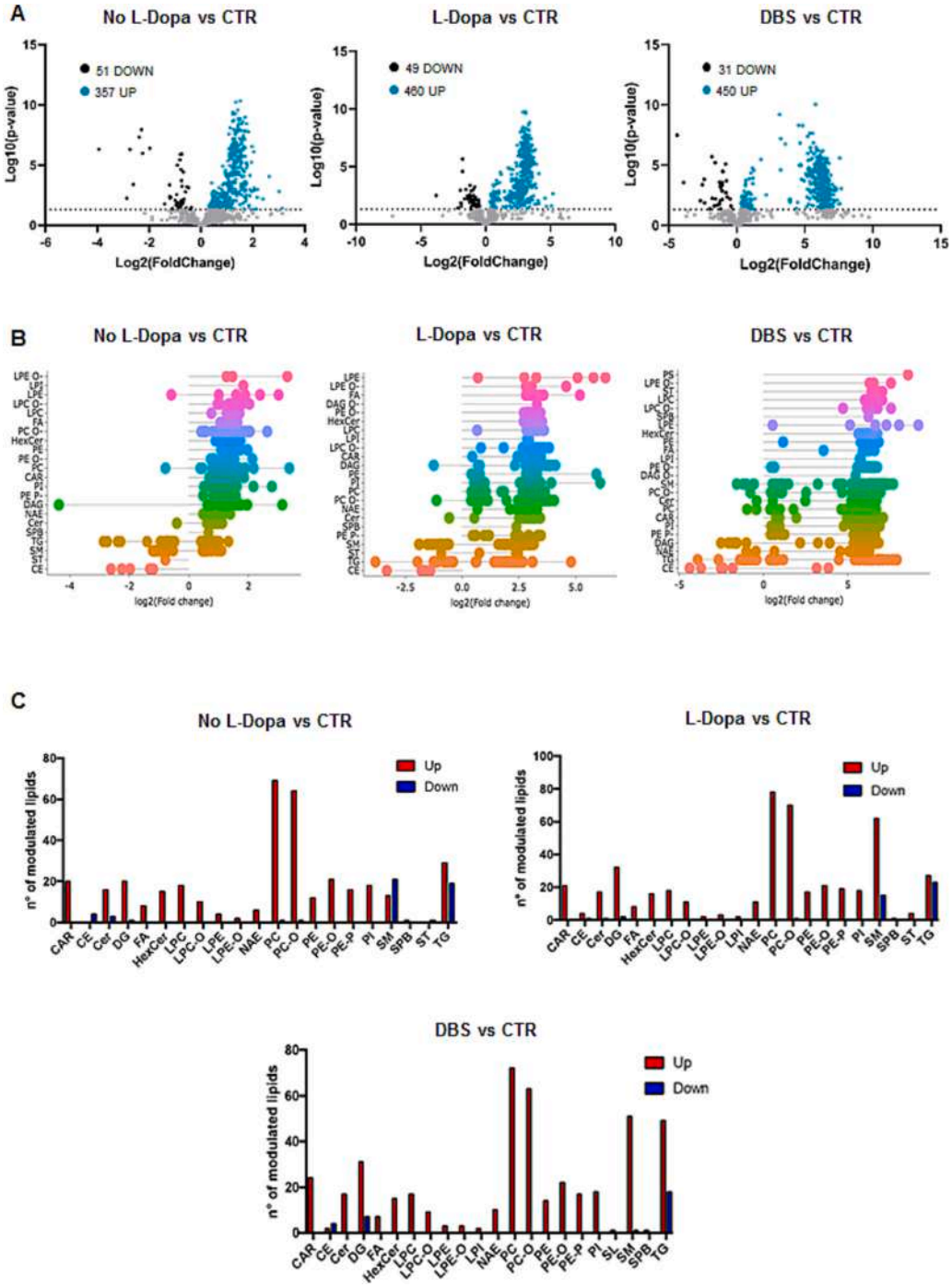

Fig. 2. Altered lipid distribution in plasma samples of PD patients. A, Volcano plot showed the distribution of the most significant altered lipid species by comparing: No L-Dopa, L-Dopa and DBS groups of patients to the control one. Lipids showing statistically significant different expression are in the top right (up-regulated) and top left (down-regulated) quadrants. The black line represents the *p*-value threshold set to $p < 0.05$. This analysis reflected a major increase, in terms of FC, in the contrasts L-Dopa and DBS patients versus controls when compared to the contrast No L-Dopa versus controls. B, Lollipop graphs represent the distribution, in term of Log2 Fold Change, of each lipid specie in the modulated lipid classes. The range of differences is higher when comparing controls with DBS patients (> -5 and < 10). C, Evaluation of the number of modulated lipid species per class. Histograms showed a comparable increase of the number of lipid species per class except for SM that showed an increased number of upregulated lipids in L-Dopa and DBS patients.

class were compared among groups (Fig. 2B).

In addition to the FC the number of species that are differentially regulated within any given class was considered, to better understand the difference of PD groups versus control (Fig. 2C). The most relevant modulated species were PC and PC-O in all the PD groups; SM species were mostly upregulated in L-Dopa and DBS versus control. Differently, a higher number of TG species were upregulated specifically in the contrast DBS versus control (Fig. 2C).

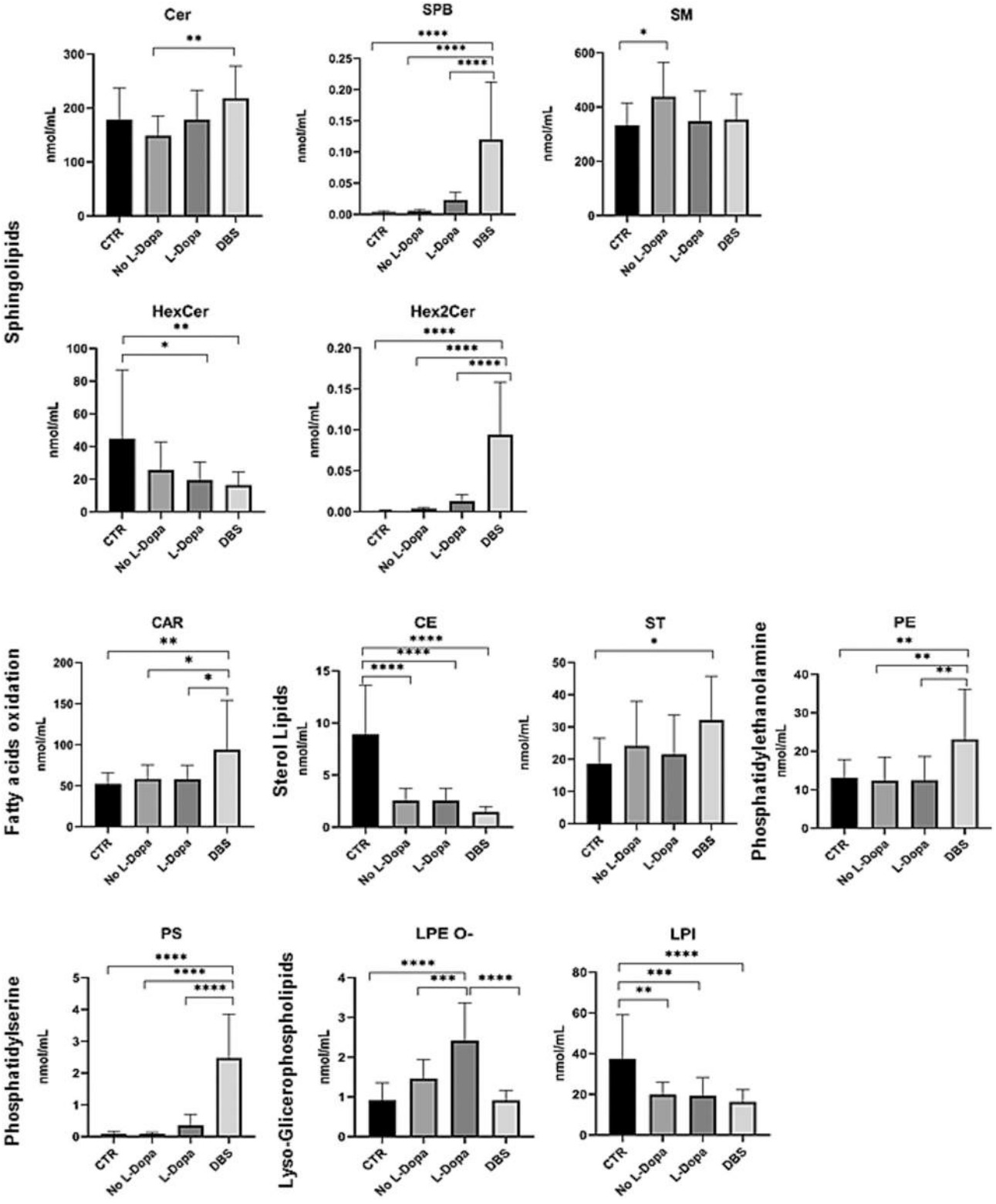

Fig. 3. Plasma concentration of the most altered lipid classes in PD patients. Comparison of plasma abundance of the 12 most dysregulated lipid classes in PD patients displayed a significant increase in all PD groups except for CE, HexCer and LPI that were reduced in all PD patients. Data are represented as mean ± SD and were analysed with one-way ANOVA and multiple comparison test. **** correspond to p-value <0.0001, *** to a p-value <0.001, ** to a p-value <0.01, * to a p-value <0.05.

Considering the abundance of measured lipids, the medium value among the concentration of the species was used to represent any given class (Fig. 3). Sphingolipids are structural molecules and important signalling mediators. Indeed, synthesis and metabolism of sphingolipids was shown to be altered in PD (Abbott et al., 2014; Bras et al., 2008) and sphingolipids increased in patients' plasma (Oizumi et al., 2022). The overall plasma concentration of sphingoid bases (2 species, C24:0, 2O and C26:0, 2O) and acylated sphingoid bases ceramides (16 species, including mostly saturated acyl species), that are inflammatory lipids, are specifically elevated in DBS, whereas their metabolite SMs are not. Further, whereas mono-glycosylated ceramides are reduced in all PD groups, Hex2Cer are significantly upregulated, reaching a highest accumulation in DBS treated plasma (Fig. 3).

Reduced levels of CARs were reported in PD patients' plasma and associated with a defect in FA oxidation (Blair et al., 2016; Ma et al., 2022; Saiki et al., 2017). Acylcarnitines alteration reflects the altered central and peripheral control of lipid metabolism. We found a significant increase of CARs in DBS patients, not only in respect with other PD groups but also with controls (Fig. 3). Although a high number of short chains was observed (58.8 % of total regulated species), the increase in plasma concentration is mainly due to medium and long chain species (Fig. 4).

Among glycerol lipids, a major representative class in plasma is PCs, with antioxidant and anti-inflammatory role (Chung et al., 2014; Murga et al., 1996; Na et al., 2015; Treede et al., 2007). We did not observe any relevant change in the mass of PC, PC-O and their de acylated forms (Fig. S3), nonetheless, PC and PC-O were profoundly remodelled with a majority of upregulated species in any PD group versus control (Fig. 2C). Similarly, SM species are majorly upregulated in the PD treated patients versus control (Fig. 2C), with no major increase in their mass, except for the untreated early PD patients (Fig. 3).

Moreover, we observed an increased ratio of PE onto LPE and a sharp increase in PE-O/ LPE-O in DBS versus all other groups (Fig. 5).

Finally, circulating TGs are known to be reduced in PD (Qiu et al., 2023). The present data indicate that TGs mass is not significantly changed in PD groups (Fig. S3) although there is a marked modulation of some TG species, especially evident in the DBS group (Figs. 1E and 2C). The ratio between TG and DG is reduced in pharmacologically treated patients but significantly increased in DBS patients (Fig. 5). At the same time, cholesterol esters are reduced in all PD patients (Fig. 3).

It is important to point out that these data remained statistically significant even if we eliminated from the analysis the two patients carrying *PRKN* mutations.

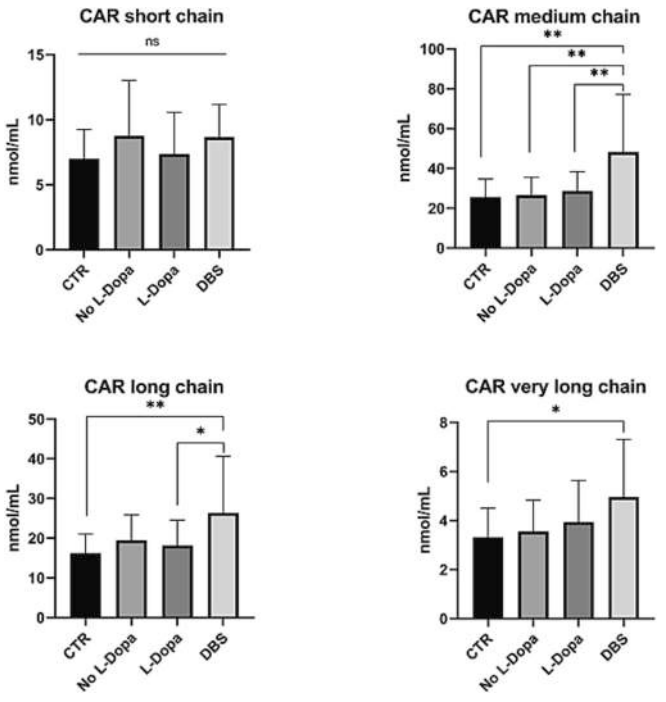

Fig. 4. Plasma concentration of short, medium, long and very long chain acylcarnitine in PD patients. Bar graphs represent the abundance of short, medium, long and very long chain acylcarnitine in PD patients. DBS patients displayed increased levels of medium, long and very long chain acylcarnitine respect to the other groups. Data are represented as mean ± SD and were analysed with one-way ANOVA and multiple comparison test. **** correspond to p-value <0.0001, *** to a p-value <0.001, ** to a p-value <0.01, * to a p-value <0.05.

3.3. Metabolomic profile in plasma samples highlighted altered amino acids metabolism in PD patients

Metabolomic analysis of circulating molecules was conducted in plasma samples of the same study cohort in which we performed lipidomic analysis to explore the presence of altered metabolic pathways, which could be associated with different disease stages and applied therapies. Hierarchical heat map, PCA and PLS-DA analyses reflected metabolic changes in all PD patients compared to control subjects (Fig. 6 A, B and Fig. S4). All PD groups of patients were well clustered based on the abundance of the molecules, suggesting the presence of a specific phenotype associated with the disease. 460 metabolites were detected and quantified in all subjects (see metabolomic dataset). We observed 105 significantly increased (FC $\geq$1.3; $p \leq 0.05$) and 89 significantly decreased molecules (FC $\leq$0.77; $p \leq 0.05$) in No L-Dopa patients with respect to controls (Fig. 6C). In L-Dopa contrast we detected 104 significantly increased and 69 significantly decreased molecules (Fig. 6C), while in DBS contrast, we found 91 significantly increased and 98 significantly decreased molecules (Fig. 6C). In PD patients we identified L-Glutamic acid, L-Histidine, L-Tryptophan, L-Tyrosine, Phenylalanine, L-Isoleucine, L-Glutamine, L-Threonine, L-Aspartic acid, L-Asparagine, L-Lysine and L-Methionine among the most significant modulated metabolites (Table 2 and Fig. S5). Interestingly, L-Glutamic acid, L-Tryptophan, L-Tyrosine, Phenylalanine and L-Glutamine were specifically decreased in the group of DBS patients (Table 2 and Fig. S5) and L-Methionine was specifically increased in the early-stage PD patients (No L-Dopa group) (Table 2 and Fig. S5). Enrichment pathway analysis, performed in KEGG database, displayed pathways specifically altered in PD patients (Fig. 7A-C), of which the majority of them were involved in the amino acid metabolism. The most significantly impacted pathways identified in all PD groups were those involved in the amino acid biosynthesis and metabolism such as Phenylalanine, tyrosine and tryptophan biosynthesis, Arginine biosynthesis, Phenylalanine metabolism, Alanine, aspartate and glutamate metabolism, Histidine metabolism, Lysine degradation but also in pathways responsible for energy production such as Glutathione metabolism, Ubiquinone biosynthesis, Pyruvate metabolism and Glycolysis and tryptophan metabolism (Behl et al., 2021; LeWitt et al., 2011; Ogawa et al., 1992) (Table 2).

3.4. Integrative correlation analysis of lipidome and metabolome of PD treatments

The correlations between lipidomics and metabolomics data were investigated using a supervised multi-omics integrative analysis which maximize the correlations between different types of omics and identify key molecules which can discriminate different sample groups. This integration was used to study the relationship between lipids and metabolites across different PD treatments.

The integrated model selected lipids and metabolites that best explain PD treatment-related variations. The general correlations between lipidome and metabolome were high (0.95 for No L-dopa, 0.75 for L-Dopa, and 0.91 for DBS, respectively), with a lower correlation in L-Dopa treated patients, suggesting the presence of common information among multi-omics results. To explore the differences in the lipid-

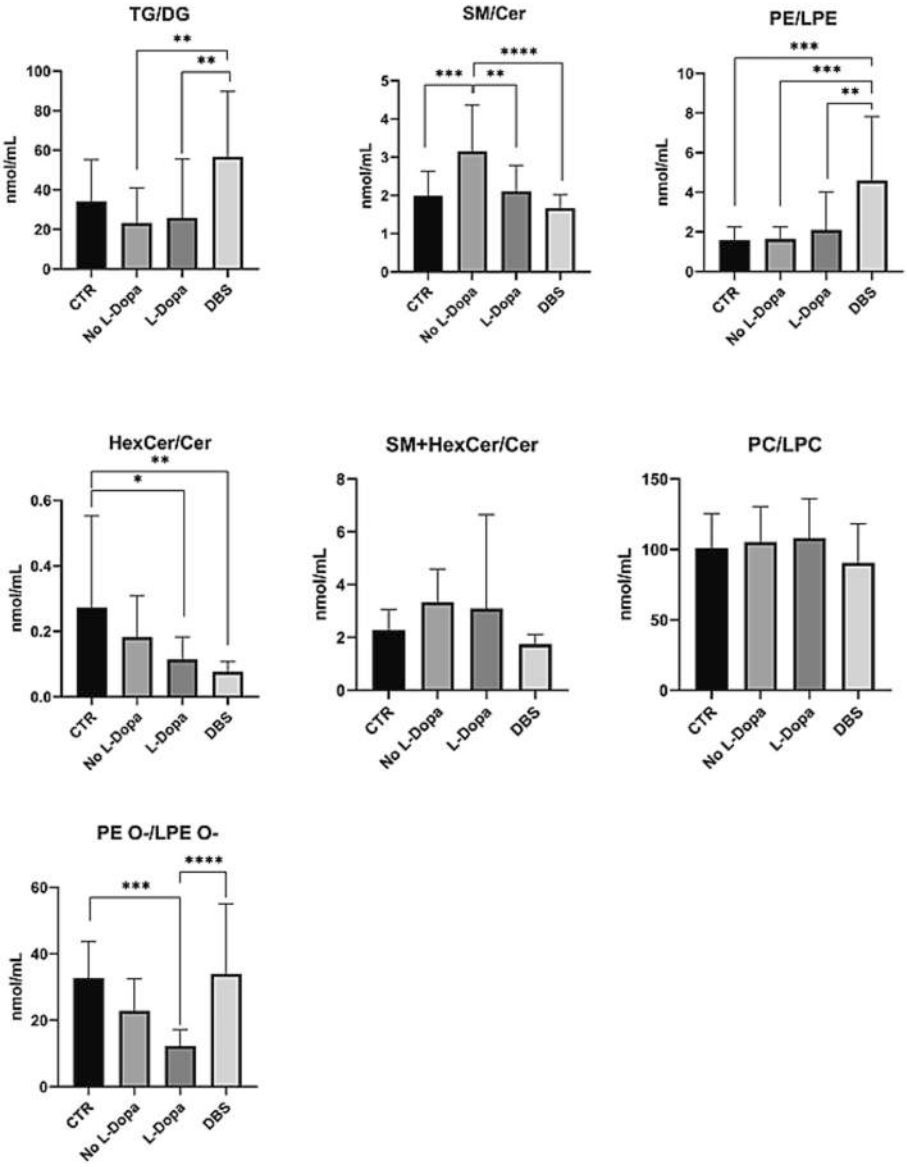

Fig. 5. Analysis of sphingolipids, glycerophospholipids and lysophospholipids ratio. Bar graphs represent the ratio of the abundance for each group of analysis. A significant increase in DBS patients was observed in the ratio TG/DG, PE/LPE and PEO/LPEO. Data are represented as mean ± SD and were analysed with one-way ANOVA and multiple comparison test. **** correspond to p-value <0.0001, *** to a p-value <0.001, ** to a p-value <0.01, * to a p-value <0.05.

metabolites association among PD treatments, we conducted a topological analysis of lipid-metabolites correlation networks (Figs. 8–10). Networks were built using all strongly correlating lipid–metabolites pairs selected in each sample group based on significant strong Pearson correlations of $r > |0.85|$. Several clusters of coregulated features strongly relevant to the latent components of the multi-omics dataset were identified, which might be a potential characteristic of PD treatments (Figs. 8–10).

The No L-Dopa patients presented a topological network with almost only positive correlations between lipids, mainly PC and LPC (LPC O-18:1, PC 0–44:5, PC 37:3|PC 17:0_20:3, PC 38:5|PC 18:0_20:5, PC 38:6, PC 39:6, PC 40:5|PC 18:0_22:5, PC O-32:0, NAE 22:4, SM 38:2;20, and SM 38:4;3O) and metabolites (niacin, butanedioic acid, acetic acid, etc.). Interestingly, two distinct networks were present, with the right one centred around PC 38:5|PC 18:0_20:5 which was positively modulated with linked metabolites (Fig. 8).

On the other hands, L-Dopa treated patients showed a network with mainly negative correlations between lipids and metabolites, with most of the molecules that were exclusively negative correlated (CAR 16:1, 4-Methaxyphenol, 4-pyridinol, Phenoxyethanol, Niacin, Levulinic acid, 1-Butanone, 3-methyl-1-phenyl-, Undecanoic acid, 2-hydroxy-2-methyl-1 phenylpropan-1-one, 4-Trimothysilyloxy −3-heptene, SM 34:2;2O, Butanedioic acid, SM 34:2;2O|SM 18:2;2O/16:0, DG 30:6, SM 40:2;20|SM 18:2;2O/22:0, PC 36:0, PI 36:4, PC 37:3, PI 38:5, DG 37:7, SM 34:2;3O, PC O-38:8, NAE 14:1, 2,5-Cyclohexadiene-1,4-dione, 2,6-bis (1,1 -dimethylethyl), 2,5-Di-tert-butyl-4-((trimethylsilyl)oxy)phenol, PC 35:4, 4-Methylvaleric acid, SM 42:3;2O|SM 18:1;2O/24;2, 3,5-di-tert-Butyl-4-hydroxyacetophenone, PC 36:4|PC 16:0_20:4, SM 38:2;2O, LPC 22:6, PC 40:6|PC 18:0_22:6, SM 43:1:2O|SM 18:1;2O/25:0, LPE O-16:1, PC O-42:5, PC O-40:4, SM 39:1;2O|SM 17:1;2O/22:0, PC 40:4, SM 36:2;2O, SM 39:1;2O, SM 42:1;2O|SM 18:1;2O/24:0, SM 44:3;2O|SM 18:1;2O/26:2, PC 39:6, PC 38:6|PC 16:0_22:6, 1-Octanol, SM 42:1:2O). Of particular interest is also the presence of few molecules that were positively correlated, namely triptophenolide, L-5-Oxoproline, 3,5-Di-tert-butyl-2-oxybenzaldehyde, anthranilic acid, and L-Tyrosine (Fig. 9).

The network analysis performed on PD patients treated with DBS showed the presence of two clusters: the first one was centred around three molecules 2,5-di-terty Butyl-1,4-benzoquinone, 11- Octadecenoic

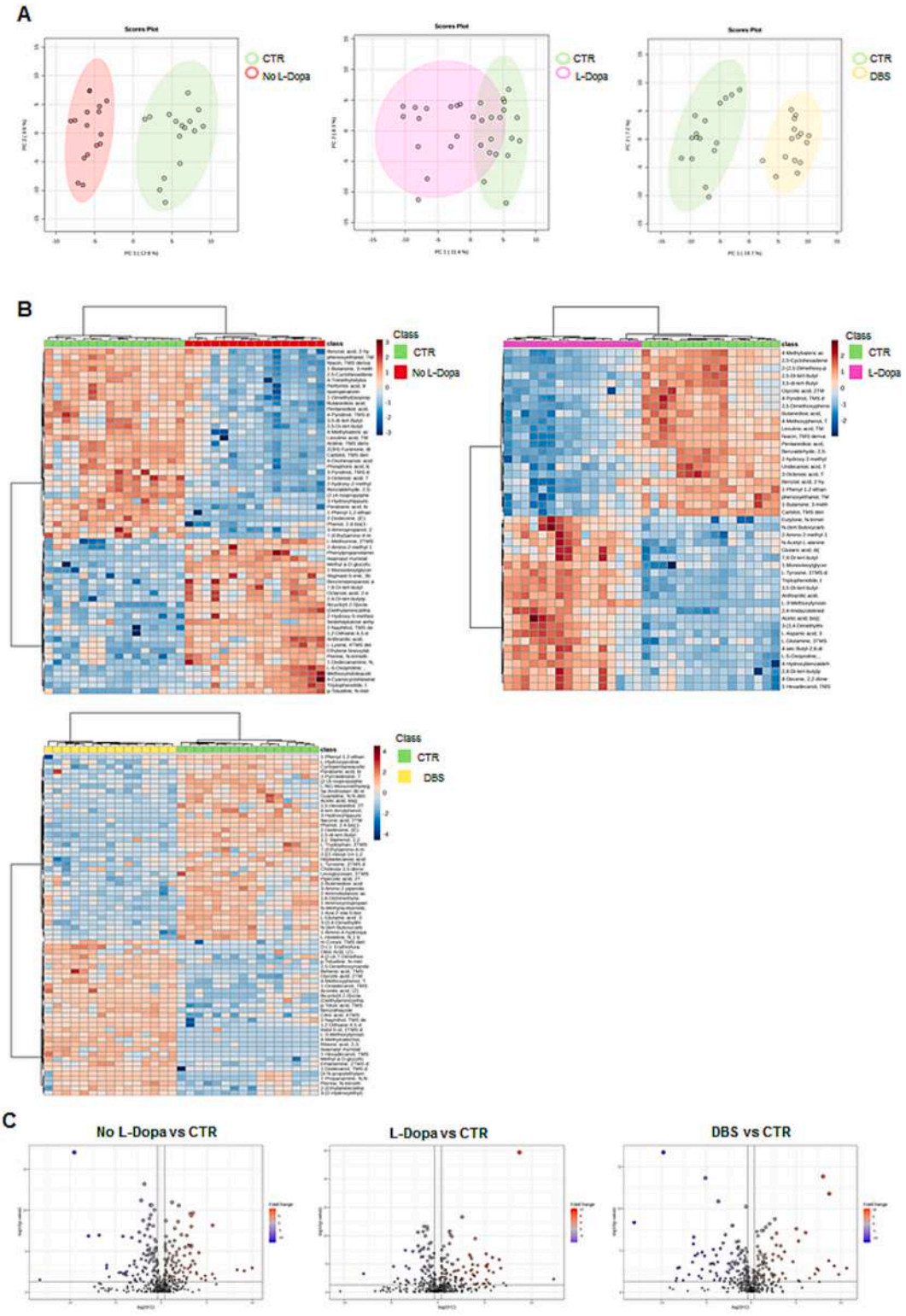

Fig. 6. Analysis of metabolomic profile in plasma samples. A, Principal Component Analysis (PCA) showed two defined group of analysis indicating differences in metabolome profile by considering No L-Dopa, L-Dopa and DBS compared to the controls. B, Heat map representation of the most significant representative metabolites displayed a discrimination between the three groups of patients compared to the controls. C, Volcano plot showed the most significant altered metabolites by comparing both PD groups vs the Control group. Red dots represented metabolites significantly up regulated while the blue dots represented the down-regulated metabolites. The black line represents the p-value threshold set to $p \leq 0.05$. (For interpretation of the references to colour in this figure legend, the reader is referred to the web version of this article.)

Table 2
Metabolites significantly modulated in plasma samples of PD patients.

		No L-Dopa vs CTR	No L-Dopa vs CTR	L-Dopa vs CTR	L-Dopa vs CTR	DBS vs CTR	DBS vs CTR
Metabolite	Pathway (KEGG)	FoldChange	p-value	FoldChange	p-value	FoldChange	p-value
L-Histidine	Histidine metabolism; beta-Alanine metabolism	0.07	0.003	0.09	0.007	0.01	2.51E-07
L-Lysine	Lysine degradation; Biotin metabolism	2.84	1.62E-08	3.23	0.0002	1.29	0.02
L-Isoleucine	Valine. leucine and isoleucine biosynthesis	0.56	0.11844	0.44	0.02	0.27	0.0004
L-Glutamic acid	Alanine. aspartate and glutamate metabolism	1.35	0.70263	14.6	0.001	0.22	1.06E-08
L-Valine	Valine. leucine and isoleucine biosynthesis; Pantothenate and CoA biosynthesis	0.82	0.51695	0.58	0.04	1.846	0.097738
L-Asparagine	Alanine. aspartate and glutamate metabolism	14.8	0.005	18.9	1.74E-05	1.71	0.32244
L-Threonine	Glycine. serine and threonine metabolism;Valine. leucine and isoleucine biosynthesis	1.19	0.33507	6.61	3.11E-05	0.45	0.2145
L-Tryptophan	Tryptophan metabolism	1.37	0.10174	2.32	0.22815	0.37	3.54E-06
L-Tyrosine	Phenylalanine, Tyrosine and Tryptophan biosynthesis	1.58	0.5	2.38	1.66E-11	0.72	1.47E-05
Phenylalanine	Phenylalanine, Tyrosine and Tryptophan biosynthesis	1.07	0.95	1.16	0.06	0.68	0.0007
L-Glutamine	Arginine biosynthesis; Purine metabolism; Pyrimidine metabolism	1.66	0.99918	11.9	1.13E-06	0.33	0.002
L-Aspartic Acid	Histidine metabolism; beta-Alanine metabolism; Pantothenate and CoA biosynthesis	3.19	0.0002	10.295	2.23E-07	0.47	1.57E-05
L-Methionine	Arginine and proline metabolism	2.38	2.29E-06	1.31	0.04	0.97	0.81

acid, and 1,2-Dithiane-4,5-diol, with the first two metabolites positively correlated with lipids and the latter negatively correlated. The second cluster was centred around 1-Butanone, 3-methyl-1-phenyl- and Niacin, with both molecules negatively correlated with lipids (Fig. 10).

Overall, this integrative analysis provided a set of multi-omics signatures for distinguishing the impact of different PD treatments and revealed correlations between lipids and metabolites within each group of analysis.

3.5. Profiling of circulating markers involved in lipid metabolism and neurodegeneration

To better explore the presence of an altered lipid metabolism in PD patients, we quantified in plasma the levels of circulating markers involved in systemic lipid metabolism (Fig. 11).

We observed a significant increase of plasma concentration of Adiponectinin in L-Dopa treated patients that was reversed in the DBS group (Fig. 11A). Moreover, Leptin concentration in plasma was reduced in PD, as previously reported (Fiszer et al., 2010), but it significatively raised up to control level, in DBS treated group (Fig. 11A). The two plasma FA transporters, FABP3 and FABP7 were reduced in PD but the DBS treated patients tended to recover a concentration of such transporters that was similar to controls (Fig. 11A). Next, we evaluated inflammatory and neurotrophic markers. The inflammatory cytokine TNF-α was significantly increased in DBS indicating the presence of inflammation, potentially associated with the surgical implant (Fig. 11B) (Meng et al., 2023). Plasma levels of glial fibrillary acidic protein (GFAP) were found to be higher in Lewy body dementia patients compared to controls (Cousins et al., 2023; Donaghy et al., 2022). In our cohort, GFAP release in plasma increased in L-Dopa versus early untreated patients, and DBS treatment almost reverted the biomarker levels to those found in the controls, suggesting a therapeutic action to counteract neurodegeneration. Nonetheless L-Dopa patients exhibit higher levels of BDNF in respect to the other PD groups (Fig. 11B).

3.6. Plasma levels of lipids, metabolites and cytokines correlated with the age at onset and with the severity of the Parkinson's disease phenotype

Correlation analysis was performed by comparing demographic (age and sex) and clinical features including age at onset (AAO), motor symptoms (UPDRS score), non-motor symptoms (NMS total score and domains D1-D7), cognitive impairment (MoCA score), L-dopa equivalent (LED) and years of disease duration, with the concentrations of 6 lipid classes (CAR, CE, CER, Hex2Cer, HexCer and SPB), three lipid species emerged by VIP analysis (TG60:14, TG60:15 and 20CE:3) and of 10 amino acids (L-Glutamic acid, L-Histidine, L-Tryptophan, L-Isoleucine, L-Glutamine, L-Threonine, L-Aspartic acid, L-Asparagine, L-Lysine, L-Methionine and L-Valine) among the most significantly modulated in PD patients. We also evaluated the levels of the circulating cytokines, analysed in this study, with PD endophenotypes.

We observed a significant negative correlation of Cer, Hex2Cer and SPB with the age at onset of the disease ($p = 0.007$; $p < 0.0001$; $p < 0.0001$; respectively) and a positive correlation with disease duration ($p = 0.001$; $p = 0.0001$; $p = 0.002$; respectively) (Fig. 12A-C). This correlation is mainly due to the DBS group of patients that showed an earlier age at onset of the disease and increased level of these lipids. CER and Hex2Cer positively correlated with the severity of non-motor symptoms domains D7 ($p = 0.01$) and D6 ($p = 0.008$), respectively (Fig. 12A, B). Hex2Cer positively correlated with LED ($r = 0.44$; $p = 0.002$).

The analysis of the selected metabolites showed a strongly significant correlation between the plasma levels of branched-chain amino acids L-isoleucine and L-valine and disease duration ($r = -0.6250$; $p < 0.0001$; $r = 0.7048$; $p < 0.0001$), as well as of L-valine with AAO ($r = -0.6795$; $p < 0.0001$) and L-isoleucine with the severity of motor symptoms (UPDRS score, $r = -0.4408$; $p = 0.003$), of non-motor symptoms (D7 domain $r = -0.4125$; $p = 0.005$) and with cognitive impairment (MoCA score, $r = 0.4171$; $p = 0.005$) (Fig. 13 A, B). The circulating levels of L-Histidine positively correlated with age at onset of the disease ($r = 0.4545$; $p = 0.001$) (Fig. 13C).

FABP7 and FABP3 increased with LED ($r = 0.4062$, $p = 0.005$; $r = 0.5430$, $p = 0.0001$; respectively) (Fig. 14 A, B). FABP7 positively correlated with the severity of motor (UPDRS, $r = 0.4419$; $p = 0.003$) and non-motor symptoms (D6; $r = 0.3997$; $p = 0.007$; D7; $r = 0.3582$; $p = 0.01$) (Fig. 14A). Increased levels of TNF-α were associated with earlier age at onset of the disease ($r = -0.3935$; $p = 0.006$) and with disease duration ($r = 0.4545$; $p = 0.001$) (Fig. 14C). Significant correlation with age was observed only with L-isoleucine and FABP7 (Figs. 13A and 14A). To adjust for age the comparison for these two markers were confirmed by multiple linear regression analysis (L-isoleucine: UPDRS, $p = 0.02$; Disease duration, $p = 0.009$; D7, $p = 0.01$; MoCA, $p = 0.02$; FABP7: LED, $p = 0.03$; UPDRS, $p = 0.02$; D6, $p = 0.03$; D7, $p = 0.04$).

From a clinical perspective, ROC analysis was performed to evaluate the diagnostic impact of the most modulated lipids, metabolites and cytokines as promising PD biomarkers. The highest performance was obtained by plotting plasma levels of Hex2Cer and SPB with the presence/absence of the disease, which resulted in sensitivity and specificity close to 100 % and fitted ROC area of 0.99 (Hex2CER) and 0.91 (SPB) (p

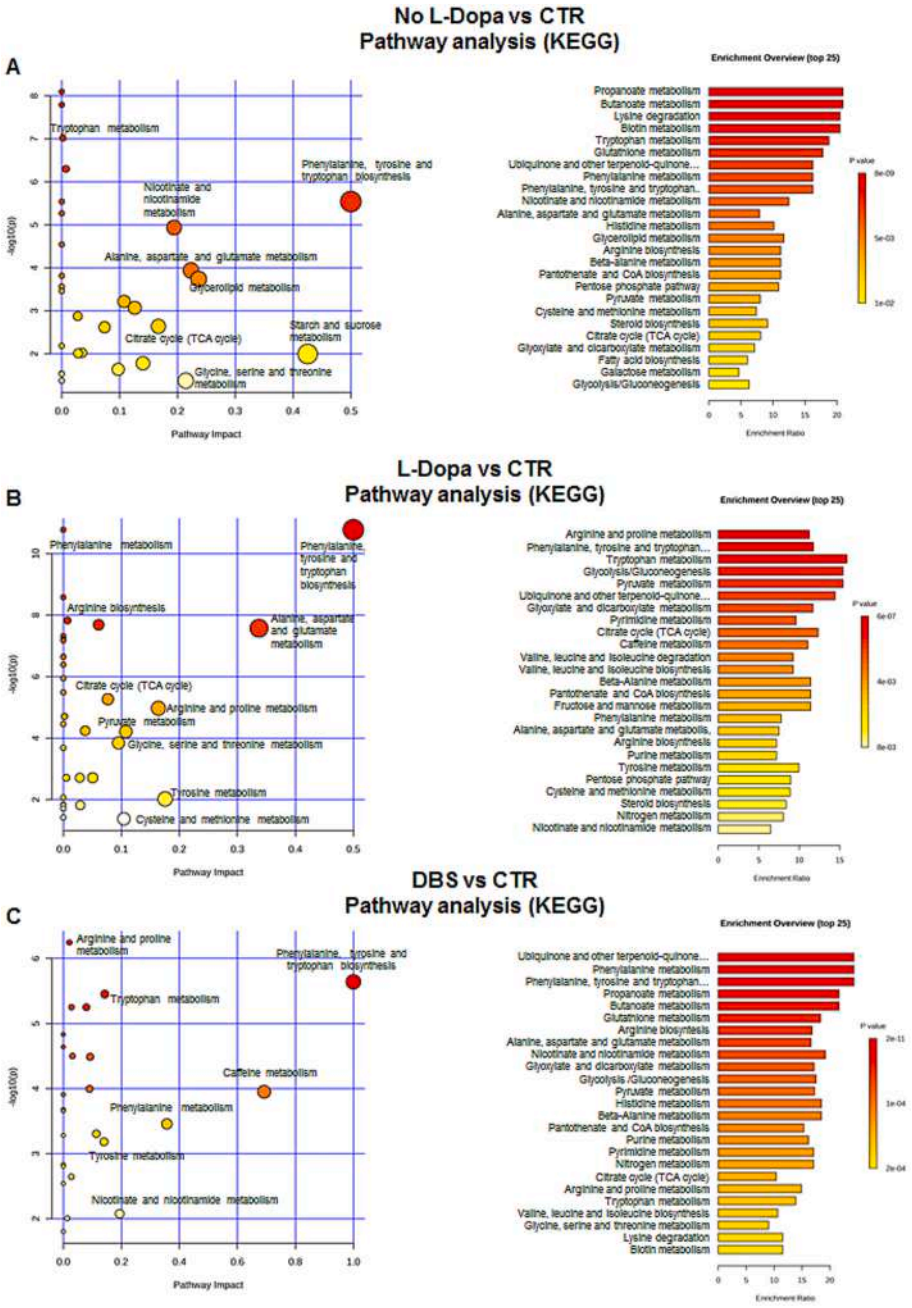

Fig. 7. Amino acids pathways dysregulation in plasma of PD patients. Metabolome view of pathway impact analysis obtained from differential metabolites in No L-Dopa (A), L-Dopa (B) and DBS (C) patients compared to the controls. Data showed an enrichment of pathways involved in amino acid metabolism and in energy production process in all PD groups analysed. The colour and size of each circle is based on *p*-values (yellow: higher p-values and red: lower p-values) and pathway impact values (the larger the circle the higher the impact score) calculated from the topological analysis, respectively. The graphs were obtained by plotting on the y-axis the -log of the *p* values from pathway enrichment analysis and on the x-axis the pathway impact values derived from pathway topology analysis. Pathways were considered significantly enriched if $p \leq 0.05$, impact 0.1 and number of metabolite hits in the pathway >1. (For interpretation of the references to colour in this figure legend, the reader is referred to the web version of this article.)

< 0.0001) (Fig. 12D). The lipid species belonging to the two lipid classes Hex2Cer and SPB identified in plasma were Hex2Cer 34:1;2O, Hex2Cer 34:2;2O, Hex2Cer 42:2;2O, SPB 24:0;2O and SPB 26:0;2O. Highly significant diagnostic accuracy was obtained by plotting data of each of five lipids (AUC: 0.99; 0.95; 0.98; 0.88; 0.92; respectively) (Fig. 12D).

4. Discussion

This is the first study adopting an untargeted omics approach to disclose alterations in PD patients associated with different disease stages and applied therapies. Our aim was to evaluate the different systemic profile of the patients, in order to evaluate how the disease and therapeutic intervention are able to modulate the body metabolism, lipid signalling and their hormonal regulation, and the inflammatory status. Thus, we compared lipidomics, metabolomics, cytokines, adipokines and lipid transporters analyses in the plasma of early PD patients, receiving Monoamine oxidase inhibitors (MAOIs) treatments, in intermediate staging L-Dopa treated patients and in late staging and DBS treated PD, compared to matched healthy subjects. Although the results of the study do not allow establishing a clear cause-effect relationship

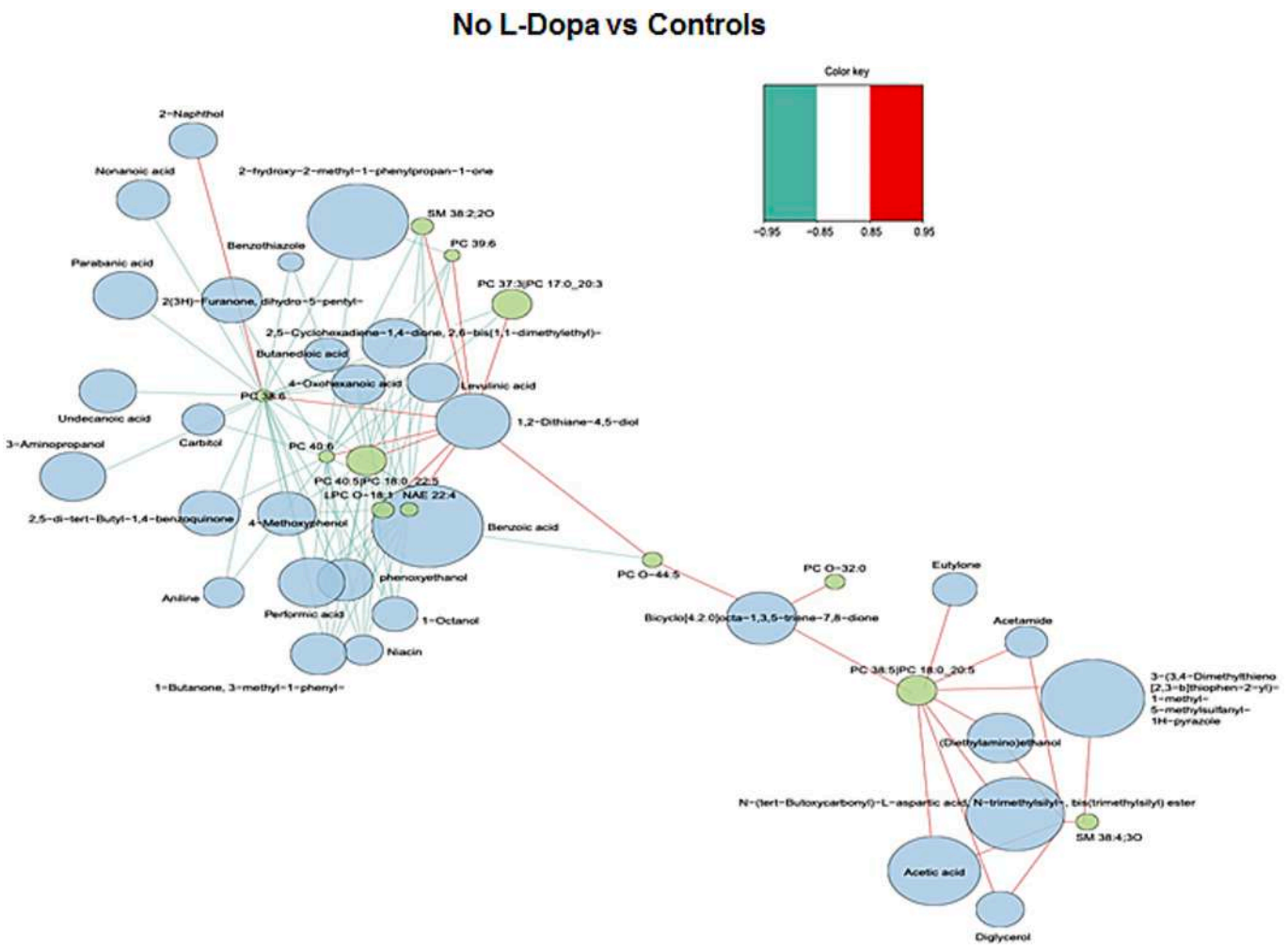

Fig. 8. Integrative correlation analysis of lipidomic and metabolomic data of No L-Dopa patients. Relevant network plot showing positive (red lines) and negative (green lines) correlations between features when comparing No L-DOPA patients with respect to controls. Correlations were calculated using Pearson correlation between each dataset. (For interpretation of the references to colour in this figure legend, the reader is referred to the web version of this article.)

depending on the therapies, due to the lack of longitudinal data, it is possible to identify lipid and metabolic profiles characteristic of the different studied groups.

Lipidomics analysis revealed a sharp modulation of plasma lipids in all analysed PD groups of patients, suggesting that this regulation is evident since the early stage of the disease. These data are in accordance with increased levels of several lipid classes associated to PD phenotype reported by other studies (Guedes et al., 2017; Li et al., 2015). The alteration of plasma lipid levels observed in PD patients could be in accordance with the involvement of lipid metabolism in PD pathogenesis (Alecu and Bennett, 2019; Ekraminasab et al., 2022; Estes et al., 2021; Fais et al., 2021). Lipids have been demonstrated to play a role in several aspects of PD pathology including specific cytotoxic interactions with α-synuclein, participation in oxidative stress and inflammation, and mutations in enzymes involved in lipid metabolism are associated with PD risk (Alecu and Bennett, 2019). By isolating the most significantly different 50 lipid species, we observed a sharp upregulation in No L-Dopa and L-Dopa compared to control that is reduced when comparing DBS versus control. This could suggest that DBS reduces the lipidome variation that is related to PD. Within the Partial Least Squares (PLS) regression, the VIP index identified a few species (11 TGs, 2 DGs, 1 CE and 1 LPE-O) that majorly predict and associate with a given group. For each specie, the score associates couples within the 4 groups, with a similar score shared by controls and DBS, and an opposite score that is similar for No L-Dopa and L-Dopa groups. Thus again, DBS modulates specific lipids, in contrast to the disease and the pharmacological treatment and overlapping with the controls. Noteworthy, changes in TG species are most relevant in identifying the groups. Long chain polyunsaturated FA, omega 3 and omega 6, are esterified in two (TG 60:14 and TG 60:15) of the 11 TG species. These two particular species, in contrast with the major bulk of TGs, are down regulated by the disease and revert to normal levels by DBS treatment. It was previously shown that circulating TGs cross the blood–brain barrier rapidly, and induce central leptin and insulin receptor resistance, decreasing satiety and cognition (Banks et al., 2018). The omega 3 and 6 storage and mobilization in the plasma may be considered as an important harm for oxidative stress defensive mechanism, given the important role of these FA in modulating neuroinflammation and in neurodegeneration (Dere Yelken et al., 2024). Another lipid that strongly associates DBS and control groups is cholesterol esterified with dihomo-γ-linolenic acid, an anti-inflammatory eicosatrienoic acid which was previously associated with insulin resistance development and cardiovascular disease (Kurotani et al., 2012; Warensjö et al., 2008). Thus, circulating storage lipids such as esterified cholesterol and triglycerides, bearing long chain unsaturated fatty acids, differentiate DBS treated patients from No L-Dopa and L-Dopa treated patients, reverting towards a control phenotype.

Considering all the species that are differentially regulated, SM and PC are profoundly remodelled in all PD patients in respect to control, in line with the implication of altered lipid metabolism in the disease

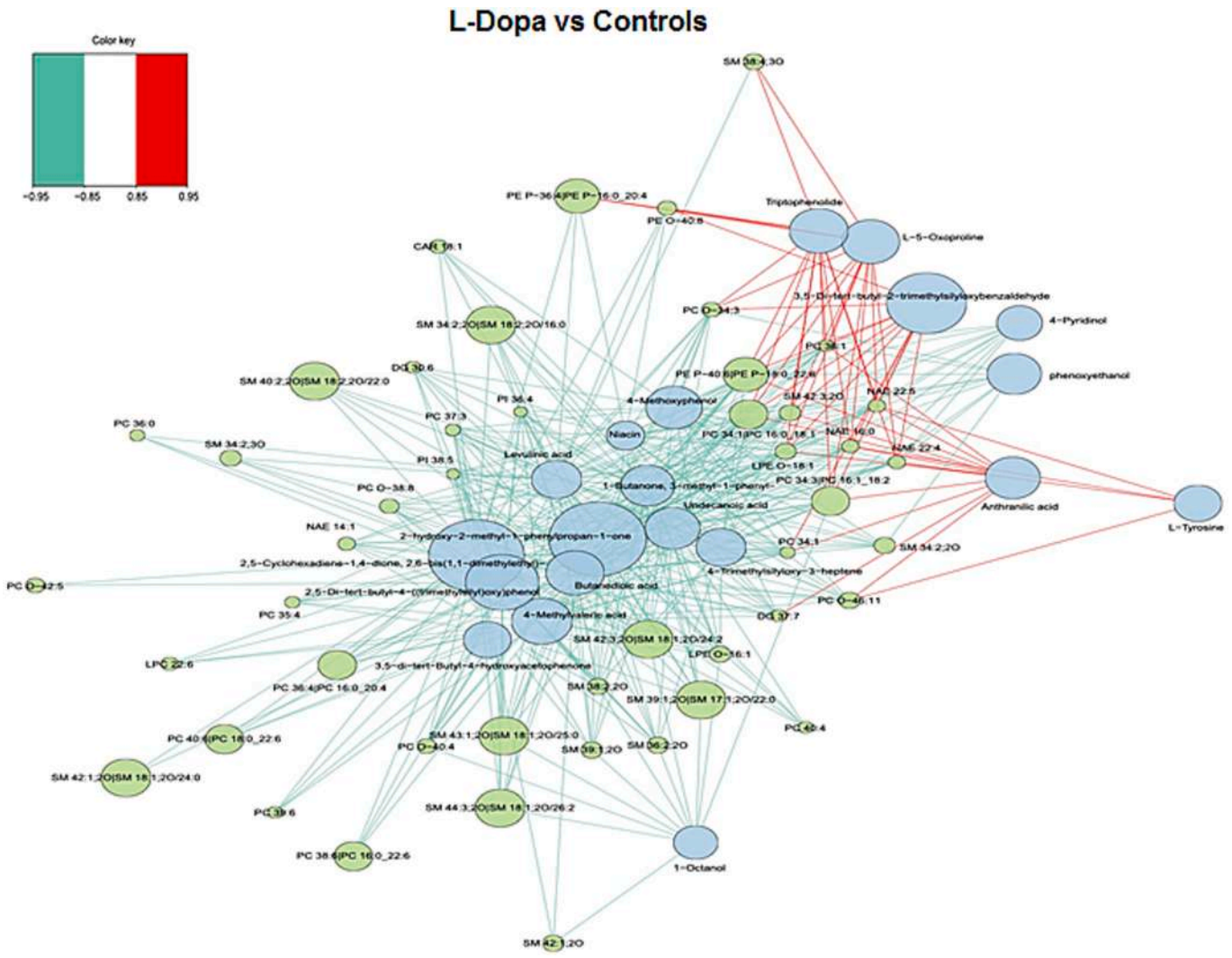

Fig. 9. Integrative correlation analysis of lipidomic and metabolomic data of L-Dopa patients. Relevant network plot showing positive (red lines) and negative (green lines) correlations between features when comparing L-DOPA patients with respect to controls. Correlations were calculated using Pearson correlation between each dataset. (For interpretation of the references to colour in this figure legend, the reader is referred to the web version of this article.)

(Alecu and Bennett, 2019; Ekraminasab et al., 2022; Estes et al., 2021; Fais et al., 2021). PC are the most abundant glycerophospholipids in cellular and mitochondrial membranes providing structural support and playing a key role in neuronal processes by affecting the differentiation of neurons and their signalling pathways. Since PCs also participate in anti-inflammatory response, their modulation in PD patients could be correlated with the inflammatory state of the disease and with the efficacy of the therapeutic approach (Dahabiyeh et al., 2023; Xicoy et al., 2019). We considered the number of species, within each class, that was significantly modulated in PD groups versus control and we observed a highest number of upregulated species of PC and PC O-, although this modulation did not change the overall mass of such lipids. Remodelling of structural lipids is a powerful defensive response from oxidative stress in neurons (Sánchez Campos et al., 2015).

DBS patients exhibited an upregulation of plasma PE, CAR, and the sphingolipids Cer, Hex2Cer, SPB in respect to controls.

CARs are closely related to mitochondrial function and energy production through the β-oxidation of FA; changes in plasma CAR concentration correlates with defects in mitochondria oxidation (Schwantje et al., 2024). In particular, we observed a significant upregulation in DBS of CAR either bearing long chain unsaturated fatty acids or short chain FA. These latter may suggest that peroxisome FA oxidation is induced in DBS patients in sustain of mitochondria oxidation (den Besten et al., 2015; Blair et al., 2016; Ma et al., 2022; Saiki et al., 2017; Stradomska et al., 2020). The increased level of CAR in DBS patients was not attributable to the presence of pathogenic mutations in PRKN, since the significance remained even when the two patients with parkin mutations were removed from the analysis.

The sphingolipids act as key factors in controlling *endo*-lysosomal pathway that is reported to be affected in PD condition (Abbott et al., 2014; Castro et al., 2014; Mielke et al., 2013; Tommasino et al., 2015). Mostly the ceramides build up in tissue and plasma under inflammatory stress and glycosylation is one of the reactions that majorly occurs to metabolise it and increase its hydrophilicity. The altered concentration of several sphingolipids was also found to correlate with PD severity as reported in previous work (Mielke et al., 2013; Taguchi et al., 2017). Increased plasma concentration of ceramides and glycosylated ceramides have been associated to cognitive decline in PD patients (Mielke et al., 2013) and Hex2Cer species increase in plasma was previously associated to Alzheimer neurodegeneration (Chua et al., 2023).

In addition we observed an important modulation of two long chains amino-alcohol, included in the sphingoid bases class (SPB,2-amino-tetracosane-1,3-diol and 2-aminodicosane 1.3 diol). The sphingoid bases are aliphatic amino alcohols that are required for all sphingolipids formation involved in numerous cellular processes including, neuronal differentiation and axonal development, cell cycle, and apoptosis

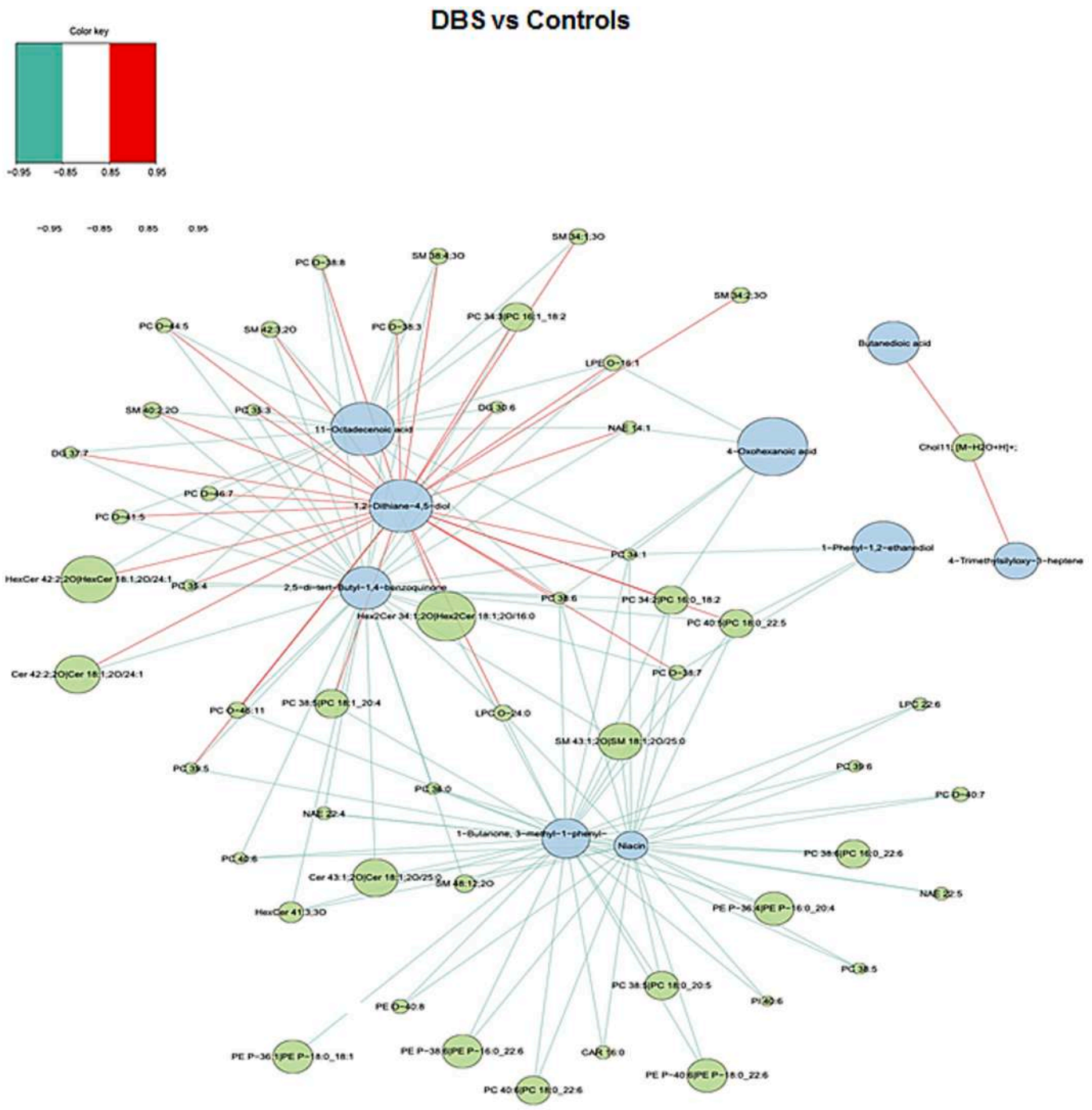

Fig. 10. Integrative correlation analysis of lipidomic and metabolomic data of DBS patients. Relevant network plot showing positive (red lines) and negative (green lines) correlations between features when comparing DBS patients with respect to controls. Correlations were calculated using Pearson correlation between each dataset. (For interpretation of the references to colour in this figure legend, the reader is referred to the web version of this article.)

(Mandik and Vos, 2021) and neurodegeneration (Goins and Spassieva, 2018). Normally SPBs derive from the condensation of Palmitate (rarely myristic and oleic acid) to serine, catalysed by Serine Palmitoyl Transferase and including a Pyridoxal phosphate dependent decarboxylation. A longer chain characterizes the two SPB species that we measured. Such species are uncommon in plasma and they have been previously detected in human urine of Alzheimers's disease affected patients (Wang et al., 2023). Acylated aminoacids are known by products of congenital fatty acids disorders, and acy-derivatives (acyl-carnitines,acyl-glycines, acyl taurines), form upon impaired mitochondria oxidation, at aim of increasing solubility to allow the blood access and urine excretion (Adeva-Andany et al., 2019). A possible reaction between fatty acids and serine, involving decarboxylation, may result in the long chain SPBs.

In particular, our findings demonstrated that increased levels of Cer, Hex2Cer and SPB in PD patients significantly correlated with earlier age at onset of the disease, with a long disease duration and with a more severe score of non-motor symptoms, for Cer and Hex2Cer. Interestingly, ROC curve analysis demonstrated that Hex2Cer and SPB lipids' classes resulted as effective biomarkers for PD.

We identify a strong increase in the number of upregulated species of SM, TG, PC and PC-O, without increasing the final mass, in the DBS group. This suggests a remodelling action that occurs to regulate specific

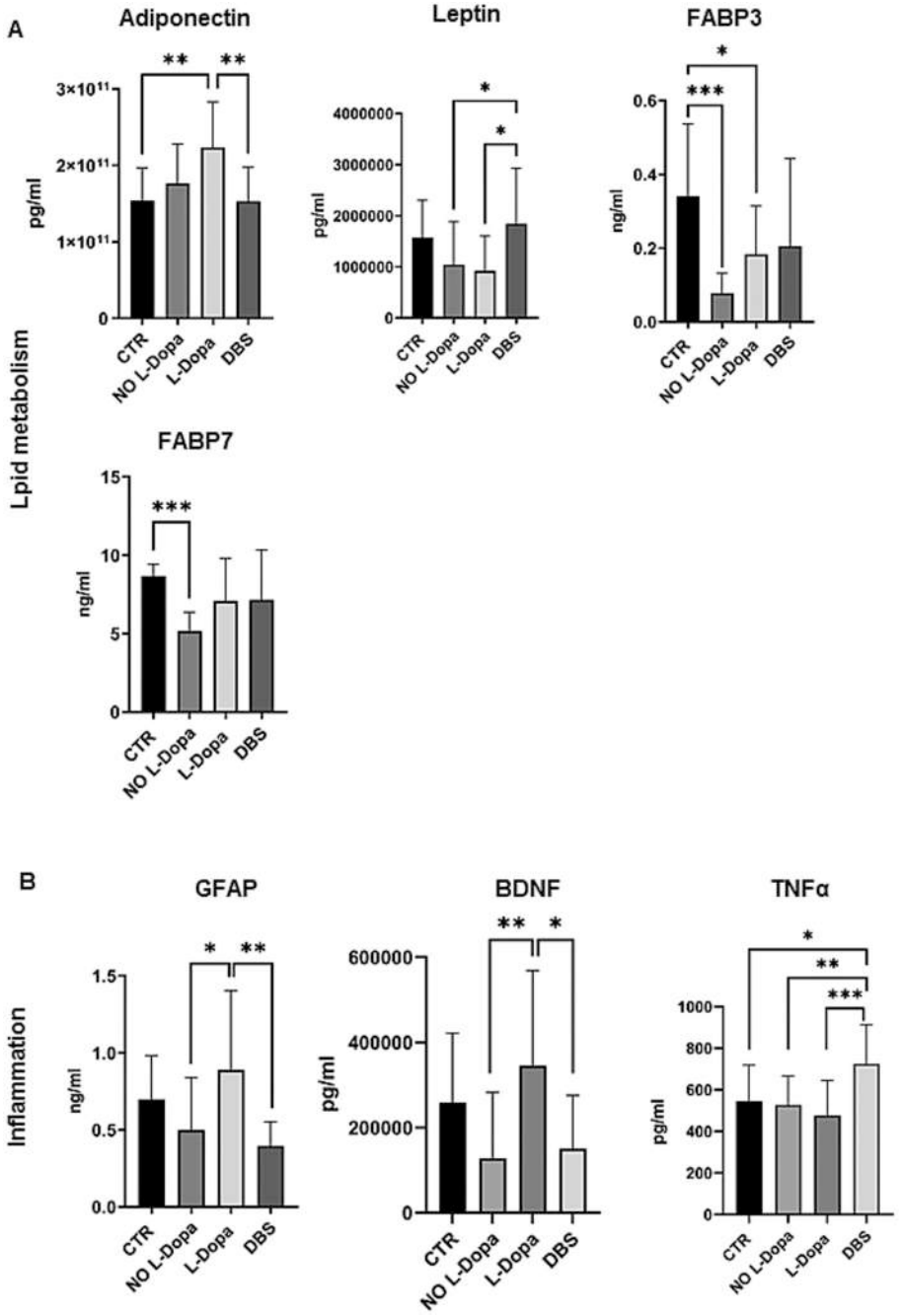

Fig. 11. Quantification of modulatory factors involved in lipid pathways and neurodegeneration. A, Graphical representation of the plasma concentration of proteins involved in lipid metabolism such as Adiponectin, Leptin, FABP3 and FABP7 in PD patients and controls. B, Graphical representation of inflammatory cytokines GFAP, BDNF and TNF-α in control (CTR), No L-Dopa, L-Dopa and DBS groups. TNF-α was significantly increased in DBS patients, while GFAP and BDNF resulted significantly increased in L-Dopa patients. Analysis was performed with one-way ANOVA and multiple comparison test. **** correspond to p-value <0.0001, *** to a p-value <0.001, ** to a p-value <0.01, * to a p-value <0.05.

substrates concentration for lipid manipulating enzymes and membranes signalling. Such changes were reported as a strategy for neural cells to protect from oxidative stress damages (Sánchez Campos et al., 2015).

The systemic lipid dysregulation that we found in PD patients was also supported by altered concentrations of proteins involved in lipid metabolism such as Adiponectin, Leptin, FABP3, FABP7 that regulate lipid function and energy balance in the different districts of the organism.

Leptin is involved in the regulation of food intake and energy expenditure through leptin receptors in hypothalamus and in the forebrain. By promoting CREB activation to sustain lipid catabolism and BDNF transcription, leptin has a neurotrophic and an antiapoptotic action (Li et al., 2021a). Leptin regulates neuroplasticity by NMDA receptor-dependent long-term depression (Durakoglugil et al., 2005) and it potentially exerts regulatory effects via the GABAergic system (Fuchs et al., 2017). Nonetheless, leptin may sustain neuroinflammation that promotes PD (Ekraminasab et al., 2022). We observed a decrease in leptin in untreated and L-Dopa treated patients and the recovery of control levels of this adipokine in the DBS group. Similarly, Markaki et al. previously observed NPY, ghrelin, and leptin secretion increases in the hypothalamus upon DBS treatment (Markaki et al., 2012).

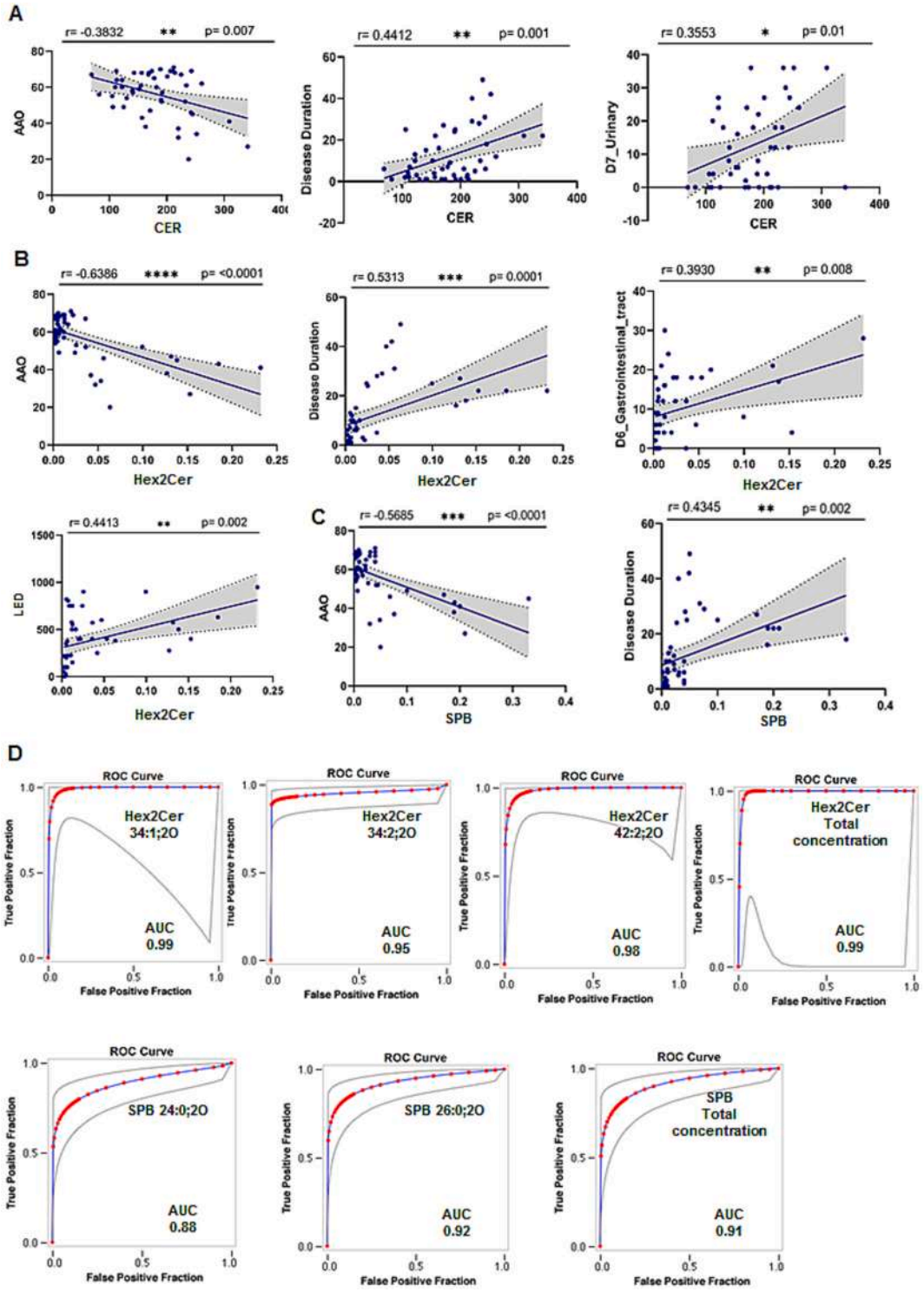

Fig. 12. Cer, Hex2Cer and SPB lipid levels correlated with age at onset and disease severity. A, Plasma levels of ceramides resulted negatively correlated with age at onset of disease (AAO) when considering all the PD patients. A positive correlation was observed with years of disease and a more severe score in urinary defects. B, Plasma levels of Hex2Cer resulted negatively correlated with AAO, while a positive correlation was observed with years of disease and gastrointestinal defects. C, Plasma levels of SPB resulted negatively correlated with AAO, while a positive correlation was observed with years of disease. D, Receiver operating characteristic (ROC) curves were calculated for the total concentrations of Hex2Cer and SPB classes as well as for the respective lipid species. Fitted area under the curves are shown in the plots.

Adiponectin is a neuroprotective adipokine, reducing inflammation, insulin resistance and oxidative stress (Rizzo et al., 2020). Adiponectin increase was observed in L-Dopa treated patients, but not in other treated or untreated groups. In association to the modulation of Adiponectin and Leptin, we observed an increase in BDNF in L-Dopa treated only opposing to a reduction trend in the other PD groups. We also observed an increase in TNF-α in the DBS treated patients only. Nonetheless, GFAP, which is powerful marker of - astrocytes inflammation (Tang et al., 2023) is actually reduced in the DBS as compared with L-Dopa, reaching a plasma concentration that is similar to the early PD

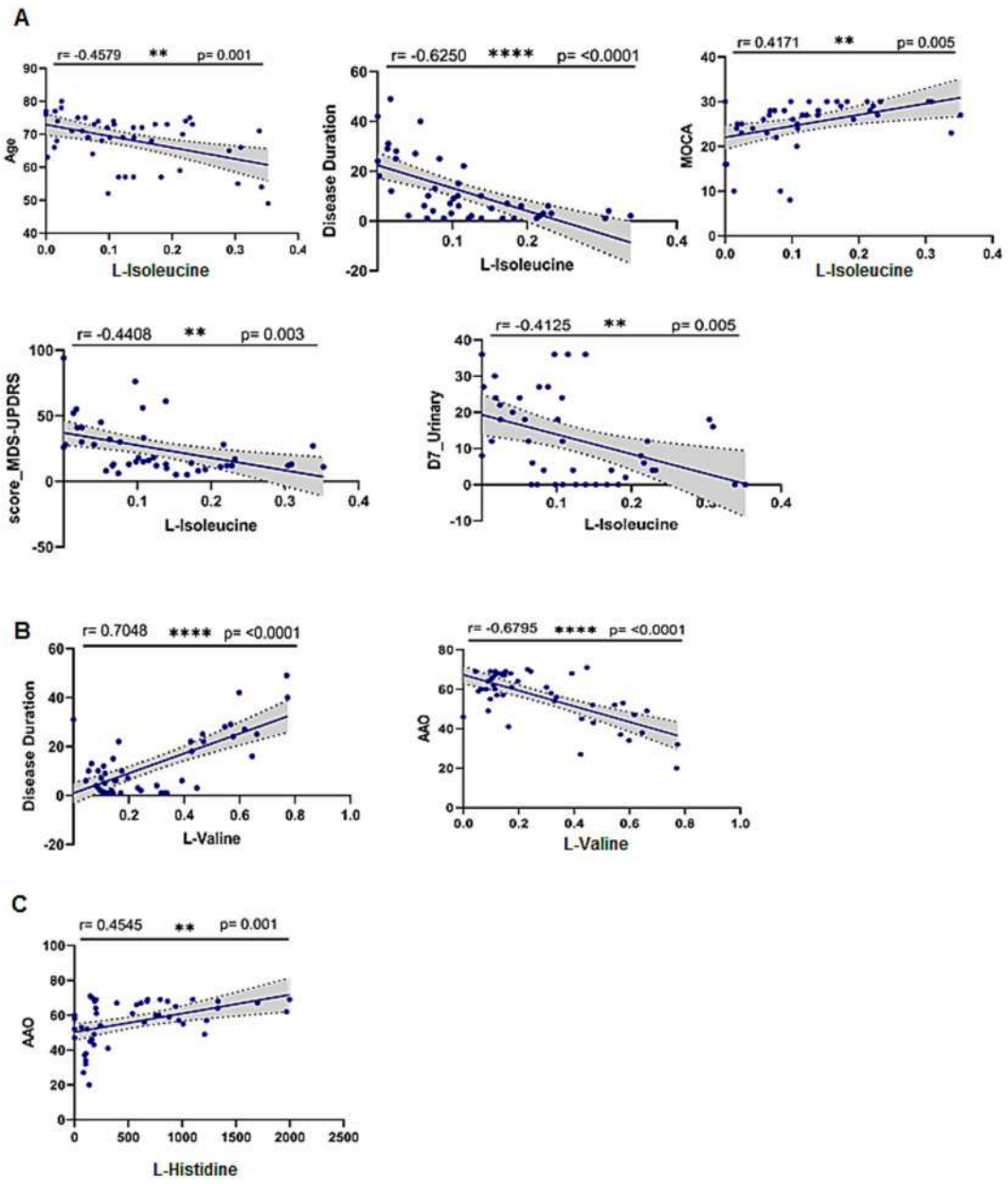

Fig. 13. Plasma levels of specific metabolites correlated with age at onset, motor and non-motor symptoms. Analysis of plasma dysregulated metabolites in PD patients. A, Decreased levels of L-Isoleucine significantly correlated with the severity of UPDRS score and with the severity of cognitive impairment (MoCA score), as well as with the severity of urinary defects. A negative correlation was observed for age and disease duration. B, Increased levels of L-Valine significantly correlated with the disease duration and with earlier age at onset. C, Graphical representation of significant positive correlation of the levels of L-Histidine with age at onset.

patients. Although DBS is known to induce an inflammatory reaction to the implant, with TNF-α and IL6 production as well as marked glial local reaction, the chronic treatment in these patients is conversely associated to antioxidant and anti-inflammatory action (Chang et al., 2023; Eser et al., 2024).

Plasma FABPs transporters ensure essential FA delivery to the brain (Pan et al., 2016): they are expressed in neurons and are involved in neuronal maturation and trophism (Xu et al., 2022). Their modulation is involved in the pathogenesis of psychiatric disorders (Shimamoto et al., 2014) and in PD neurodegeneration (Kawahata et al., 2023). We observed reduced levels of FABP3 and 7 in early and in L-Dopa PD groups, whereas DBS treatment induces a weak but consistent recover of both plasma FA transporters. Thus, DBS promotes lipid remodelling and their mobilization through local and systemic effects that are regulated by hormones and lipid related proteins, potentially adding to the therapeutic benefit and offering new markers for therapy monitoring. New approaches are now exploring the possibility to engage electro stimulation without invasiveness by exploiting trans cranial application of the stimulus. The challenge is now to identify what biological mechanism are responsible of DBS therapeutic effects and if they can be reproduced by trans cranial electrical stimulation.

At metabolomic level, we found a wide dysregulation of pathways involved in the biosynthesis and metabolism of several amino acids such as phenylalanine, tyrosine, tryptophan, arginine, alanine, histidine, aspartate and glutamate.

Interestingly, L-threonine, L-tryptophan, L-glutamine, L-aspartic acid, L-Tyrosine, Phenylalanine and L-glutamic acid showed a slight increase in early stage (No L-Dopa) PD patients, a highly significant increase in the L-Dopa group of patients and a completely different profile in DBS patients in which they were significantly decreased

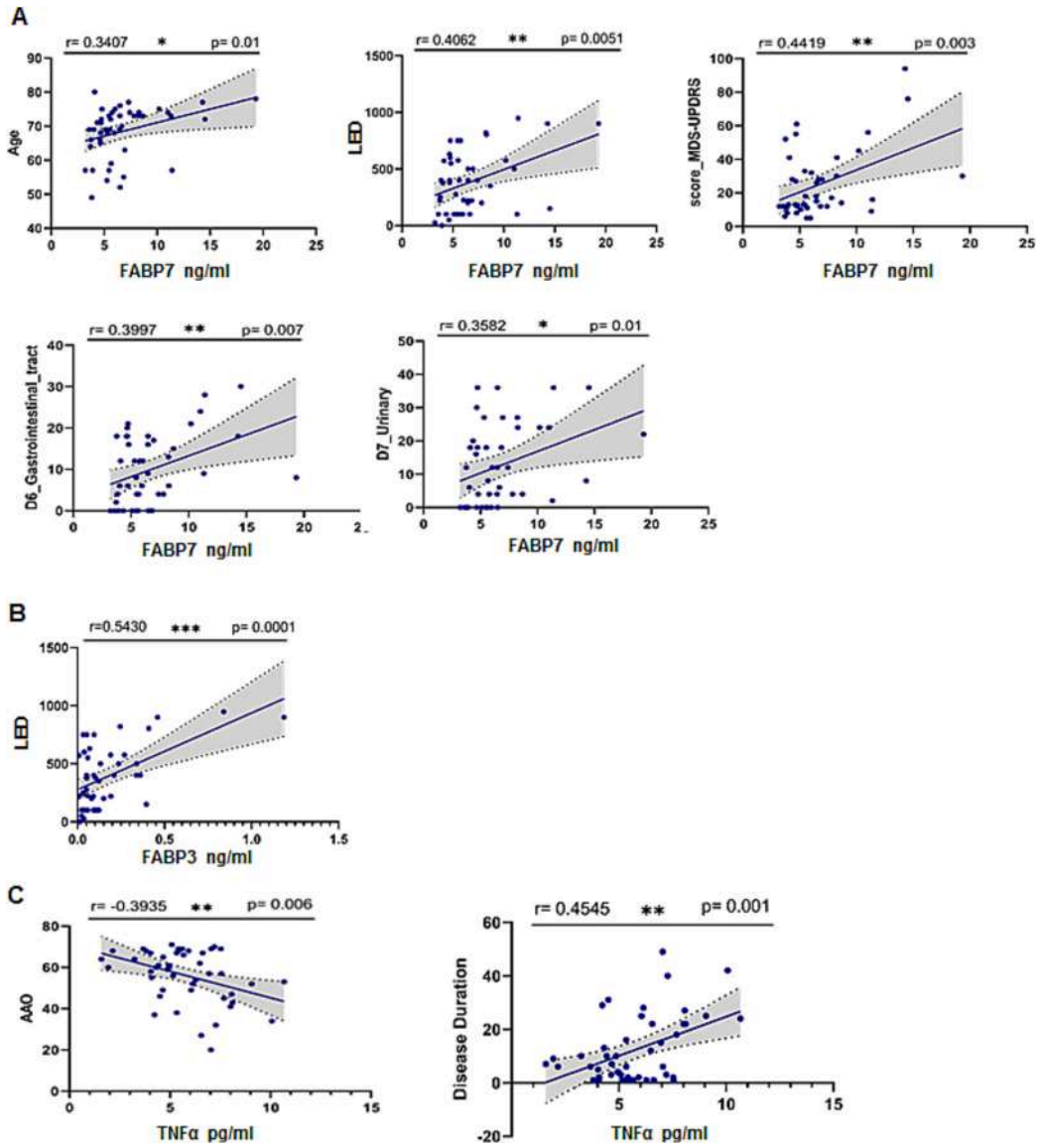

Fig. 14. Correlation analysis of modulatory factors involved in lipid pathways and neurodegeneration with disease endophenotypes. A, FABP7 positively correlated with the age, the severity of motor symptoms (UPDRS scores) and with gastrointestinal and urinary defects (D6 and D7), as well as with increased dosage of L-Dopa therapy (LED). B, Increased levels of FABP3 were associated with increased dosage of L-Dopa therapy (LED). C, Increased levels of TNF-α were associated with earlier age at onset of the disease and positively correlated with the years of the disease.

compared to controls, suggesting that the levels of these amino acids might change with disease therapy.

It is well known that dietary habits affect PD symptoms, progression, and overall health (Earp et al., 2023). Our results highlighted circulating amino acid alterations in PD patients, suggesting that the development of a precision nutritional supplement that targets specific amino acids could have a beneficial impact on patients. Such supplementation should be designed to minimize interference with levodopa medication, while providing nutrients to correct amino acid deficiencies (Wu et al., 2024). A monocentric, prospective, randomized, double-blind pilot study performed on two groups of Parkinson-affected patients reported that amino acid supplementation did not show detrimental effects on neurological and pharmacological control in patients chronically treated with L-dopa. Furthermore, daily amino acid supplementation partially counteracted insulin resistance development and the loss in antioxidant availability (Cucca et al., 2015). Therefore, more studies on specific amino acid supplementation should be designed.

It was particularly interesting to observe that DBS patients showed a highly significant reduction of circulating levels of L-glutamic acid, suggesting that this therapy could have a beneficial impact on the activation of glutamatergic cascade. These results are in accordance with the role of L-glutamic acid in neurodegenerative diseases, in fact, excessive synthesis or release of L-glutamate and the reduction of its reuptake led to a high concentration of L-glutamate in the synaptic space resulting in toxicity and neuronal death (Li et al., 2021b). Moreover, there are many studies that suggest that the abnormal aggregation of alpha-synuclein in PD is closely related to enhance the excitatory toxicity of glutamic acid, which may be a potential neuropathological pathway (Gu et al., 2010; Sarafian et al., 2017; Wang et al., 2020; Yang et al., 2016).

Integration analysis of lipidomics and metabolomics data disclose several modulated molecules involved in glutathione metabolism and in neurodegeneration. It is known that glutathione, a tripeptide consisting of cysteine, glutamic acid and glycine, plays an important role as a cell signalling molecule involved in the regulation of apoptosis, cell cycling, immunity and it participates in active transcellular amino acid transport. In abnormal conditions, the absence or low glycine levels do not allow the formation of glutathione, leading an increase to the production

of glutamic acid and L-5-oxoproline levels and an ATP-depleting (Emmett, 2014). Specifically, the accumulation of L-5-oxoproline, as we observed in both early PD and L-dopa PD patients (Table S1, Fig. 8 and metabolomic dataset), causes neurotoxicity, oxidative stress and production of reactive species (Pederzolli et al., 2010). Our data also showed an increase of pyroglutamic acid and glutamic acid levels at the early-stage PD, thus correlated with symptoms worsening and a decrease of Niacin levels (Table S1). The L-Dopa treatment didn't impact their levels, while in DBS patients the concentrations of L-5-oxoproline and Niacin returned to values comparable with control patients, and the levels of glutamic acid decreased significantly (Table S1 and Table 2). Those results could indicate that the DBS treatment, in addition to reducing energy depleting, might be involved in glutathione metabolism.

Another interesting molecule was Pterin. Pterins play important role as cofactors and they are involved in Phenylalanine and Tyrosine metabolism to produce Dopamine, and a dysregulation of Pterin levels can lead to alterations in neurotransmitter production, impairing neuronal capacities (Eichwald et al., 2023).

Our data showed a significant decreased of Phenylalanine and L-Tyrosine levels in DBS patients compared to control and a significant increase of Pterin and Homovanillic acid levels compared to control patients (Table S1). Interestingly, increase of Homovanillic acid in CSF of mild stage Parkinson's disease patients was already correlated with motor impairment (Stefani et al., 2017).

Moreover, we observed a significant increase in oleic acid in the DBS group compared to the control: as already showed by Heller et al., oleic acid can trigger dopamine production by stimulating dopaminergic activity (Heller et al., 2005; Xicoy et al., 2019).

Finally, the integrative analysis highlighted a different impact of the treatments on the lipidome and the metabolome. While not treated patients presented almost only positive correlations between phospholipids and metabolites, the L-Dopa treatment reversed the relationship between lipids and molecules showing mainly negative correlations between them, while the DBS treatment reported the presence of both positively and negatively correlated lipid-metabolites clusters. These findings demonstrate the complexity of lipid-molecules interactions in different PD treatments.

5. Limitations of the study

This pilot study presents several limitations that include the size of the study sample, the lack of longitudinal data to assess the impact of the different treatments on lipidomic and metabolomic profile, as well as the different genetic and molecular background of the PD cohort. Replication in a larger cohort is required to validate these results. Moreover, it must be considered that the differences in metabolic markers that we observe are associated with groups of patients that differentiate not only for the therapeutic treatments but also for their disease staging.

The No-L Dopa patients are at an early stage of the disease and treated with different therapeutics such as MAO inhibitors and/or Dopa agonists; the L-Dopa patients are at middle stage of disease and treated with L-Dopa, often flanked with MAO inhibitors and/or Dopa agonists; the DBS patients are at an advanced stage of disease and received long time treatment with L-Dopa and other drugs, switching to a later treatment of L-Dopa in addiction to DBS implantation. Moreover, since PD may be considered a systemic disease, the observed biochemical variations could be attributable to changes in the metabolism of peripheral organs and/or pharmacological treatment, rather than DBS. Nonetheless, we noticed that lipid and metabolite profiles are able to cluster the specific groups.

6. Conclusions

Overall, these data, although require further investigations in larger cohorts, highlights new findings in metabolic alterations in PD patients, PD progression and severity as well as the impact of different PD treatments.

Consent for publication

Not applicable.

Author contributions

TE, PS and MM designed the study. NM, SP, TG, MS, TB, AP and NPP recruited the patients, performed clinical study, and collected the data. NPP performed sample management and bio banking. MG, CD, EB and MM performed lipidomic and metabolomic analysis. SK and MM performed integration analysis. FC, GF, MG, CD, EB, MM and TE performed bioinformatic and statistical analysis of omics data. FC and TE performed the correlation analyses. FC, TE, MM and PS wrote the manuscript. All authors revised the final manuscript.

CRediT authorship contribution statement

Federica Carrillo: Writing – review & editing, Writing – original draft, Investigation, Data curation. **Nicole Piera Palomba:** Investigation, Data curation. **Marco Ghirimoldi:** Investigation, Formal analysis. **Camilla Didò:** Investigation, Formal analysis. **Giorgio Fortunato:** Investigation. **Shahzaib Khoso:** Formal analysis. **Tiziana Giloni:** Investigation, Data curation. **Marco Santilli:** Investigation, Data curation. **Tommaso Bocci:** Investigation. **Alberto Priori:** Investigation. **Sara Pietracupa:** Investigation, Data curation. **Nicola Modugno:** Investigation, Data curation. **Elettra Barberis:** Investigation, Formal analysis. **Marcello Manfredi:** Writing – review & editing, Investigation, Funding acquisition, Formal analysis, Data curation, Conceptualization. **Paola Signorelli:** Writing – review & editing, Investigation, Funding acquisition, Formal analysis, Data curation, Conceptualization. **Teresa Esposito:** Writing – review & editing, Writing – original draft, Supervision, Investigation, Funding acquisition, Formal analysis, Data curation, Conceptualization.

Declaration of competing interest

The authors declare that they have no known competing financial interests or personal relationships that could have appeared to influence the work reported in this paper.

Data availability

All data are available in the main text or the supplementary materials. The datasets used and/or analysed during the current study are available as metabolomic and lipidomic datasets.

Acknowledgements

We are grateful to the Italian Ministry of Health was supported this work by grant n. PNRR-MAD-2022-12375960 Next Generation EU - PNRR M6C2 Investimento 2.1 valorizzazione e potenziamento della ricerca biomedica del SSN to TE, grant n. RF 2019-12370224 to TE, and Current Research to TE. We also thank Italian Ministry of University and Research (M.U.R) that supported by the project PRIN n. 2022W3RKLJ funded by European Union – Next Generation EU and by CNR project FOE-2021 DBA.AD005.225. FC was supported by Italian Ministry of University and Research (M.U.R) project CIR01_00023 - IMPARA - IMAGING DALLE MOLECOLE ALLA PRECLINICA – PNIR – Programma Nazionale Infrastrutture di Ricerca. This study was (partially) funded by the Italian Ministry of University and Research (MUR) program "Departments of Excellence 2023-2027", AGING Project – Department of Translational Medicine, Università del Piemonte Orientale. The study was partly supported by a donation in memory of Aldo Ravelli ('Aldo

Ravelli' Research Center for Neurotechnology and Experimental Neurotherapeutics).

The funders had no role in study design, data collection and analysis, decision to publish, or preparation of the manuscript.

Appendix A. Supplementary data

Supplementary data to this article can be found online at https://doi.org/10.1016/j.nbd.2024.106698.

References

Abbott, S.K., Li, H., Muñoz, S.S., Knoch, B., Batterham, M., Murphy, K.E., et al., 2014. Altered ceramide acyl chain length and ceramide synthase gene expression in Parkinson's disease. Mov. Disord. 29, 518–526. https://doi.org/10.1002/mds.25729.

Adeva-Andany, M.M., Carneiro-Freire, N., Seco-Filgueira, M., Fernández-Fernández, C., Mouriño-Bayolo, D., 2019. Mitochondrial β-oxidation of saturated fatty acids in humans. Mitochondrion 46, 73–90. https://doi.org/10.1016/j.mito.2018.02.009.

Alecu, I., Bennett, S.A.L., 2019. Dysregulated lipid metabolism and its role in α-synucleinopathy in Parkinson's disease. Front. Neurosci. 13. https://doi.org/10.3389/fnins.2019.00328.

Angeli, A., Mencacci, N.E., Duran, R., Aviles-Olmos, I., Kefalopoulou, Z., Candelario, J., et al., 2013. Genotype and phenotype in Parkinson's disease: lessons in heterogeneity from deep brain stimulation. Mov. Disord. 28, 1370–1375. https://doi.org/10.1002/mds.25535.

Avenali, M., Zangaglia, R., Cuconato, G., Palmieri, I., Albanese, A., Artusi, C.A., et al., 2023. Are patients with GBA–Parkinson disease good candidates for deep brain stimulation? A longitudinal multicentric study on a large Italian cohort. J. Neurol. Neurosurg. Psychiatry. https://doi.org/10.1136/jnnp-2023-332387 jnnp-2023-332387.

Aybek, S., Gronchi-Perrin, A., Berney, A., Chiuvé, S.C., Villemure, J., Burkhard, P.R., et al., 2007. Long-term cognitive profile and incidence of dementia after STN-DBS in Parkinson's disease. Mov. Disord. 22, 974–981. https://doi.org/10.1002/mds.21478.

Banks, W.A., Farr, S.A., Salameh, T.S., Niehoff, M.L., Rhea, E.M., Morley, J.E., et al., 2018. Triglycerides cross the blood–brain barrier and induce central leptin and insulin receptor resistance. Int. J. Obes. 42, 391–397. https://doi.org/10.1038/ijo.2017.231.

Barberis, E., Timo, S., Amede, E., Vanella, V.V., Puricelli, C., Cappellano, G., et al., 2020. Large-scale plasma analysis revealed new mechanisms and molecules associated with the host response to SARS-CoV-2. Int. J. Mol. Sci. 21, 8623. https://doi.org/10.3390/ijms21228623.

Barberis, E., Amede, E., Tavecchia, M., Marengo, E., Cittone, M.G., Rizzi, E., et al., 2021. Understanding protection from SARS-CoV-2 using metabolomics. Sci. Rep. 11, 13796. https://doi.org/10.1038/s41598-021-93260-2.

Behl, T., Kaur, I., Sehgal, A., Singh, S., Bhatia, S., Al-Harrasi, A., et al., 2021. The footprint of kynurenine pathway in neurodegeneration: Janus-faced role in Parkinson's disorder and therapeutic implications. Int. J. Mol. Sci. 22, 6737. https://doi.org/10.3390/ijms22136737.

Blair, H.C., Sepulveda, J., Papachristou, D.J., 2016. Nature and nurture in atherosclerosis: the roles of acylcarnitine and cell membrane-fatty acid intermediates. Vasc. Pharmacol. 78, 17–23. https://doi.org/10.1016/j.vph.2015.06.012.

Bloem, B.R., Okun, M.S., Klein, C., 2021. Parkinson's disease. Lancet 397, 2284–2303. https://doi.org/10.1016/S0140-6736(21)00218-X.

Bras, J., Singleton, A., Cookson, M.R., Hardy, J., 2008. Emerging pathways in genetic Parkinson's disease: potential role of ceramide metabolism in Lewy body disease. FEBS J. 275, 5767–5773. https://doi.org/10.1111/j.1742-4658.2008.06709.x.

Castro, B.M., Prieto, M., Silva, L.C., 2014. Ceramide: a simple sphingolipid with unique biophysical properties. Prog. Lipid Res. 54, 53–67. https://doi.org/10.1016/j.plipres.2014.01.004.

Chang, L., Dong, W., Luo, B., Qiu, C., Lu, Y., Lin, X., et al., 2023. Deep brain stimulation improves central nervous system inflammation in Parkinson's disease: evidence and perspectives. CNS Neurosci. Ther. 29, 2177–2185. https://doi.org/10.1111/cns.14167.

Chua, X.Y., Torta, F., Chong, J.R., Venketasubramanian, N., Hilal, S., Wenk, M.R., et al., 2023. Lipidomics profiling reveals distinct patterns of plasma sphingolipid alterations in Alzheimer's disease and vascular dementia. Alzheimers Res. Ther. 15, 214. https://doi.org/10.1186/s13195-023-01359-7.

Chung, S.J., Lee, C.H., Lee, H.S., Kim, S.T., Sohn, U.D., Park, E.S., et al., 2014. The role of phosphatidylcholine and deoxycholic acid in inflammation. Life Sci. 108, 88–93. https://doi.org/10.1016/j.lfs.2014.05.013.

Coelho, M., Marti, M.J., Sampaio, C., Ferreira, J.J., Valldeoriola, F., Rosa, M.M., et al., 2015. Dementia and severity of parkinsonism determines the handicap of patients in late-stage Parkinson's disease: the Barcelona–Lisbon cohort. Eur. J. Neurol. 22, 305–312. https://doi.org/10.1111/ene.12567.

Cousins, K.A.Q., Irwin, D.J., Chen-Plotkin, A., Shaw, L.M., Arezoumandan, S., Lee, E.B., et al., 2023. Plasma GFAP associates with secondary Alzheimer's pathology in Lewy body disease. Ann. Clin. Transl. Neurol. 10, 802–813. https://doi.org/10.1002/acn3.51768.

Cucca, A., Mazzucco, S., Bursomanno, A., Antonutti, L., Di Girolamo, F.G., Pizzolato, G., et al., 2015. Amino acid supplementation in l-dopa treated Parkinson's disease patients. Clin. Nutr. 34, 1189–1194. https://doi.org/10.1016/j.clnu.2014.12.007.

Dahabiyeh, L.A., Nimer, R.M., Rashed, M., Wells, J.D., Fiehn, O., 2023. Serum-based lipid panels for diagnosis of idiopathic Parkinson's disease. Metabolites 13, 990. https://doi.org/10.3390/metabo13090990.

den Besten, G., Gerding, A., van Dijk, T.H., Ciapaite, J., Bleeker, A., van Eunen, K., et al., 2015. Protection against the metabolic syndrome by guar gum-derived Short-chain fatty acids depends on peroxisome proliferator-activated receptor γ and glucagon-like Peptide-1. PLoS One 10, e0136364. https://doi.org/10.1371/journal.pone.0136364.

Dere Yelken, H., Elci, M.P., Turker, P.F., Demirkaya, S., 2024. Omega fatty acid ratios and neurodegeneration in a healthy environment. Prostaglandins Other Lipid Mediat. 170, 106799. https://doi.org/10.1016/j.prostaglandins.2023.106799.

Donaghy, P.C., Firbank, M., Petrides, G., Lloyd, J., Barnett, N., Olsen, K., et al., 2022. The relationship between plasma biomarkers and amyloid PET in dementia with Lewy bodies. Parkinsonism Relat. Disord. 101, 111–116. https://doi.org/10.1016/j.parkreldis.2022.07.008.

Durakoglugil, M., Irving, A.J., Harvey, J., 2005. Leptin induces a novel form of NMDA receptor-dependent long-term depression. J. Neurochem. 95, 396–405. https://doi.org/10.1111/j.1471-4159.2005.03375.x.

Earp, J.E., Colon-Semenza, C., LoBuono, D.L., 2023. Considerations for developing a targeted amino acid supplement for people with Parkinson's disease that promotes health while accounting for pathophysiology and medication interference. Nutr. Rev. 81, 1063–1076. https://doi.org/10.1093/nutrit/nuad008.

Eichwald, T., da Silva, L., da Staats Pires ACS, B., Niero, L., Schnorrenberger, E., Filho, C. C., et al., 2023. Tetrahydrobiopterin: beyond its traditional role as a cofactor. Antioxidants 12, 1037. https://doi.org/10.3390/antiox12051037.

Ekraminasab, S., Dolatshahi, M., Sabahi, M., Mardani, M., Rashedi, S., 2022. The interactions between adipose tissue secretions and Parkinson's disease: the role of leptin. Eur. J. Neurosci. 55, 873–891. https://doi.org/10.1111/ejn.15594.

Emmett, M., 2014. Acetaminophen toxicity and 5-Oxoproline (Pyroglutamic acid). Clin. J. Am. Soc. Nephrol. 9, 191–200. https://doi.org/10.2215/CJN.07730713.

Eser, P., Kocabicak, E., Bekar, A., Temel, Y., 2024. Insights into neuroinflammatory mechanisms of deep brain stimulation in Parkinson's disease. Exp. Neurol. 374, 114684. https://doi.org/10.1016/j.expneurol.2024.114684.

Espay, A.J., Brundin, P., Lang, A.E., 2017. Precision medicine for disease modification in Parkinson disease. Nat. Rev. Neurol. 13, 119–126. https://doi.org/10.1038/nrneurol.2016.196.

Estes, R.E., Lin, B., Khera, A., Davis, M.Y., 2021. Lipid metabolism influence on neurodegenerative disease progression: is the vehicle as important as the cargo? Front. Mol. Neurosci. 14. https://doi.org/10.3389/fnmol.2021.788695.

Fais, M., Dore, A., Galioto, M., Galleri, G., Crosio, C., Iaccarino, C., 2021. Parkinson's disease-related genes and lipid alteration. Int. J. Mol. Sci. 22, 7630. https://doi.org/10.3390/ijms22147630.

Fanning, S., Selkoe, D., Dettmer, U., 2020. Parkinson's disease: proteinopathy or lipidopathy? NPJ Parkinsons Dis. 6. https://doi.org/10.1038/s41531-019-0103-7.

Fiszer, U., Michałowska, M., Baranowska, B., Wolińska-Witort, E., Jeske, W., Jethon, M., et al., 2010. Leptin and ghrelin concentrations and weight loss in Parkinson's disease. Acta Neurol. Scand. 121, 230–236. https://doi.org/10.1111/j.1600-0404.2009.01185.x.

Fuchs, T., Jefferson, S.J., Hooper, A., Yee, P.-H., Maguire, J., Luscher, B., 2017. Disinhibition of somatostatin-positive GABAergic interneurons results in an anxiolytic and antidepressant-like brain state. Mol. Psychiatry 22, 920–930. https://doi.org/10.1038/mp.2016.188.

Gialluisi, A., Reccia, M.G., Tirozzi, A., Nutile, T., Lombardi, A., De Sanctis, C., et al., 2020. Whole exome sequencing study of Parkinson disease and related Endophenotypes in the Italian population. Front. Neurol. 10. https://doi.org/10.3389/fneur.2019.01362.

Gialluisi, A., Reccia, M.G., Modugno, N., Nutile, T., Lombardi, A., Di Giovannantonio, L. G., et al., 2021. Identification of sixteen novel candidate genes for late onset Parkinson's disease. Mol. Neurodegener. 16. https://doi.org/10.1186/s13024-021-00455-2.

Goins, L., Spassieva, S., 2018. Sphingoid bases and their involvement in neurodegenerative diseases. Adv. Biol. Regul. 70, 65–73. https://doi.org/10.1016/j.jbior.2018.10.004.

Gu, X.-L., Long, C.-X., Sun, L., Xie, C., Lin, X., Cai, H., 2010. Astrocytic expression of Parkinson's disease-related A53T α-synuclein causes neurodegeneration in mice. Mol. Brain 3, 12. https://doi.org/10.1186/1756-6606-3-12.

Guedes, L.C., Chan, R.B., Gomes, M.A., Conceição, V.A., Machado, R.B., Soares, T., et al., 2017. Serum lipid alterations in GBA-associated Parkinson's disease. Parkinsonism Relat. Disord. 44, 58–65. https://doi.org/10.1016/j.parkreldis.2017.08.026.

Hartmann, C.J., Fliegen, S., Groiss, S.J., Wojtecki, L., Schnitzler, A., 2019. An update on best practice of deep brain stimulation in Parkinson's disease. Ther. Adv. Neurol. Disord. 12. https://doi.org/10.1177/1756286419838096, 175628641983809.

Heller, A., Won, L., Bubula, N., Hessefort, S., Kurutz, J.W., Reddy, G.A., et al., 2005. Long-chain fatty acids increase cellular dopamine in an immortalized cell line (MN9D) derived from mouse mesencephalon. Neurosci. Lett. 376, 35–39. https://doi.org/10.1016/j.neulet.2004.11.021.

Hellstrand, E., Grey, M., Ainalem, M.-L., Ankner, J., Forsyth, V.T., Fragneto, G., et al., 2013. Adsorption of α-Synuclein to supported lipid bilayers: positioning and role of electrostatics. ACS Chem. Neurosci. 4, 1339–1351. https://doi.org/10.1021/cn400066t.

Ikenaka, K., Suzuki, M., Mochizuki, H., Nagai, Y., 2019. Lipids as trans-acting effectors for α-Synuclein in the pathogenesis of Parkinson's disease. Front. Neurosci. 13. https://doi.org/10.3389/fnins.2019.00693.

Kawahata, I., Sekimori, T., Oizumi, H., Takeda, A., Fukunaga, K., 2023. Using fatty acid-binding proteins as potential biomarkers to discriminate between Parkinson's disease and dementia with Lewy bodies: exploration of a novel technique. Int. J. Mol. Sci. 24, 13267. https://doi.org/10.3390/ijms241713267.

Kurotani, K., Sato, M., Ejima, Y., Nanri, A., Yi, S., Pham, N.M., et al., 2012. High levels of stearic acid, palmitoleic acid, and dihomo-γ-linolenic acid and low levels of linoleic acid in serum cholesterol ester are associated with high insulin resistance. Nutr. Res. 32, 669–675.e3. https://doi.org/10.1016/j.nutres.2012.07.004.

Kurzawa-Akanbi, M., Tammireddy, S., Fabrik, I., Gliaudelytė, L., Doherty, M.K., Heap, R., et al., 2021. Altered ceramide metabolism is a feature in the extracellular vesicle-mediated spread of alpha-synuclein in Lewy body disorders. Acta Neuropathol. 142, 961–984. https://doi.org/10.1007/s00401-021-02367-3.

Le, W., Pan, T., Huang, M., Xu, P., Xie, W., Zhu, W., et al., 2008. Decreased NURR1 gene expression in patients with Parkinson's disease. J. Neurol. Sci. 273, 29–33. https://doi.org/10.1016/j.jns.2008.06.007.

LeWitt, P., Schultz, L., Auinger, P., Lu, M., 2011. CSF xanthine, homovanillic acid, and their ratio as biomarkers of Parkinson's disease. Brain Res. 1408, 88–97. https://doi.org/10.1016/j.brainres.2011.06.057.

Li, Z., Zhang, J., Sun, H., 2015. Increased plasma levels of phospholipid in Parkinson's disease with mild cognitive impairment. J. Clin. Neurosci. 22, 1268–1271. https://doi.org/10.1016/j.jocn.2015.02.013.

Li, T., Yang, Z., Li, S., Cheng, C., Shen, B., Le, W., 2018. Alterations of NURR1 and cytokines in the peripheral blood mononuclear cells: combined biomarkers for Parkinson's disease. Front. Aging Neurosci. 10. https://doi.org/10.3389/fnagi.2018.00392.

Li, C., Meng, F., Lei, Y., Liu, J., Liu, J., Zhang, J., et al., 2021a. Leptin regulates exon-specific transcription of the Bdnf gene via epigenetic modifications mediated by an AKT/p300 HAT cascade. Mol. Psychiatry 26, 3701–3722. https://doi.org/10.1038/s41380-020-00922-0.

Li, X., Wang, W., Yan, J., Zeng, F., 2021b. Glutamic acid transporters: targets for neuroprotective therapies in Parkinson's disease. Front. Neurosci. 15. https://doi.org/10.3389/fnins.2021.678154.

Liu, M.Y., Xydakis, A.M., Hoogeveen, R.C., Jones, P.H., Smith, E.O., Nelson, K.W., et al., 2005. Multiplexed analysis of biomarkers related to obesity and the metabolic syndrome in human plasma, using the Luminex-100 system. Clin. Chem. 51, 1102–1109. https://doi.org/10.1373/clinchem.2004.047084.

Ma, Y., Wang, M., Guo, S., Li, T., Liu, X., Zhao, L., 2022. The serum acylcarnitines profile in epileptic children treated with valproic acid and the protective roles of peroxisome proliferator-activated receptor a activation in valproic acid-induced liver injury. Front. Pharmacol. 13. https://doi.org/10.3389/fphar.2022.1048728.

Mandik, F., Vos, M., 2021. Neurodegenerative disorders: spotlight on sphingolipids. Int. J. Mol. Sci. 22, 11998. https://doi.org/10.3390/ijms222111998.

Markaki, E., Ellul, J., Kefalopoulou, Z., Trachani, E., Theodoropoulou, A., Kyriazopoulou, V., et al., 2012. The role of ghrelin, neuropeptide Y and leptin peptides in weight gain after deep brain stimulation for Parkinson's disease. Stereotact. Funct. Neurosurg. 90, 104–112. https://doi.org/10.1159/000335045.

Meng, H., Wei, J.-H., Yu, P.-Z., Ren, J.-X., Tang, M.-Y., Sun, J.-Y., et al., 2023. Insights into advanced neurological dysfunction mechanisms following DBS surgery in Parkinson's patients: Neuroinflammation and Pyroptosis. Curr. Issues Mol. Biol. 45, 4480–4494. https://doi.org/10.3390/cimb45050284.

Merola, A., Zibetti, M., Angrisano, S., Rizzi, L., Lanotte, M., Lopiano, L., 2011. Comparison of subthalamic nucleus deep brain stimulation and Duodopa in the treatment of advanced Parkinson's disease. Mov. Disord. 26, 664–670. https://doi.org/10.1002/mds.23524.

Mielke, M.M., Maetzler, W., Haughey, N.J., Bandaru, V.V.R., Savica, R., Deuschle, C., et al., 2013. Plasma ceramide and glucosylceramide metabolism is altered in sporadic Parkinson's disease and associated with cognitive impairment: a pilot study. PLoS One 8, e73094. https://doi.org/10.1371/journal.pone.0073094.

Murga, C., Ruiz-Gómez, A., García-Higuera, I., Kim, C.M., Benovic, J.L., Mayor, F., 1996. High affinity binding of β-adrenergic receptor kinase to microsomal membranes. J. Biol. Chem. 271, 985–994. https://doi.org/10.1074/jbc.271.2.985.

Na, J.-Y., Song, K., Kim, S., Kwon, J., 2015. Hepatoprotective effect of phosphatidylcholine against carbon tetrachloride liver damage in mice. Biochem. Biophys. Res. Commun. 460, 308–313. https://doi.org/10.1016/j.bbrc.2015.03.031.

Ogawa, T., Matson, W.R., Beal, M.F., Myers, R.H., Bird, E.D., Milbury, P., et al., 1992. Kynurenine pathway abnormalities in Parkinson's disease. Neurology 42, 1702. https://doi.org/10.1212/WNL.42.9.1702.

Oizumi, H., Sugimura, Y., Totsune, T., Kawasaki, I., Ohshiro, S., Baba, T., et al., 2022. Plasma sphingolipid abnormalities in neurodegenerative diseases. PLoS One 17, e0279315. https://doi.org/10.1371/journal.pone.0279315.

Palomba, N.P., Fortunato, G., Pepe, G., Modugno, N., Pietracupa, S., Damiano, I., et al., 2023. Common and rare variants in TMEM175 gene concur to the pathogenesis of Parkinson's disease in Italian patients. Mol. Neurobiol. 60, 2150–2173. https://doi.org/10.1007/s12035-022-03203-9.

Pan, Y., Short, J.L., Choy, K.H.C., Zeng, A.X., Marriott, P.J., Owada, Y., et al., 2016. Fatty Acid-Binding Protein 5 at the blood–brain barrier regulates endogenous brain docosahexaenoic acid levels and cognitive function. J. Neurosci. 36, 11755–11767. https://doi.org/10.1523/JNEUROSCI.1583-16.2016.

Pederzolli, C.D., Mescka, C.P., Zandoná, B.R., de Moura, Coelho D., Sgaravatti, Â.M., Sgarbi, M.B., et al., 2010. Acute administration of 5-oxoproline induces oxidative damage to lipids and proteins and impairs antioxidant defenses in cerebral cortex and cerebellum of young rats. Metab. Brain Dis. 25, 145–154. https://doi.org/10.1007/s11011-010-9190-1.

Postuma, R.B., Berg, D., Stern, M., Poewe, W., Olanow, C.W., Oertel, W., et al., 2015. MDS clinical diagnostic criteria for Parkinson's disease. Mov. Disord. 30, 1591–1601. https://doi.org/10.1002/mds.26424.

Qiu, J., Wei, L., Su, Y., Tang, Y., Peng, G., Wu, Y., et al., 2023. Lipid metabolism disorder in cerebrospinal fluid related to Parkinson's disease. Brain Sci. 13, 1166. https://doi.org/10.3390/brainsci13081166.

Rizzo, M.R., Fasano, R., Paolisso, G., 2020. Adiponectin and Cognitive Decline. Int. J. Mol. Sci. 21, 2010. https://doi.org/10.3390/ijms21062010.

Saiki, S., Hatano, T., Fujimaki, M., Ishikawa, K.I., Mori, A., Oji, Y., et al., 2017. Decreased long-chain acylcarnitines from insufficient β-oxidation as potential early diagnostic markers for Parkinson's disease. Sci. Rep. 7. https://doi.org/10.1038/s41598-017-06767-y.

Sánchez Campos, S., Rodríguez Diez, G., Oresti, G.M., Salvador, G.A., 2015. Dopaminergic neurons respond to Iron-induced oxidative stress by modulating lipid acylation and Deacylation cycles. PLoS One 10, e0130726. https://doi.org/10.1371/journal.pone.0130726.

Sarafian, T.A., Littlejohn, K., Yuan, S., Fernandez, C., Cilluffo, M., Koo, B., et al., 2017. Stimulation of synaptoneurosome glutamate release by monomeric and fibrillated α-synuclein. J. Neurosci. Res. 95, 1871–1887. https://doi.org/10.1002/jnr.24024.

Schwantje, M., Mosegaard, S., Knottnerus, S.J.G., van Klinken, J.B., Wanders, R.J., van Lenthe, H., et al., 2024. Tracer-based lipidomics enables the discovery of disease-specific candidate biomarkers in mitochondrial β-oxidation disorders. FASEB J. 38. https://doi.org/10.1096/fj.202302163R.

Shahmoradian, S.H., Lewis, A.J., Genoud, C., Hench, J., Moors, T.E., Navarro, P.P., et al., 2019. Lewy pathology in Parkinson's disease consists of crowded organelles and lipid membranes. Nat. Neurosci. 22, 1099–1109. https://doi.org/10.1038/s41593-019-0423-2.

Shao, Y., Li, T., Liu, Z., Wang, X., Xu, X., Li, S., et al., 2021. Comprehensive metabolic profiling of Parkinson's disease by liquid chromatography-mass spectrometry. Mol. Neurodegener. 16, 4. https://doi.org/10.1186/s13024-021-00425-8.

Shimamoto, C., Ohnishi, T., Maekawa, M., Watanabe, A., Ohba, H., Arai, R., et al., 2014. Functional characterization of FABP3, 5 and 7 gene variants identified in schizophrenia and autism spectrum disorder and mouse behavioral studies. Hum. Mol. Genet. 23, 6495–6511. https://doi.org/10.1093/hmg/ddu369.

Singh, A., Shannon, C.P., Gautier, B., Rohart, F., Vacher, M., Tebbutt, S.J., et al., 2019. DIABLO: an integrative approach for identifying key molecular drivers from multi-omics assays. Bioinformatics 35, 3055–3062. https://doi.org/10.1093/bioinformatics/bty1054.

Stefani, A., Pierantozzi, M., Olivola, E., Galati, S., Cerroni, R., D'Angelo, V., et al., 2017. Homovanillic acid in CSF of mild stage Parkinson's disease patients correlates with motor impairment. Neurochem. Int. 105, 58–63. https://doi.org/10.1016/j.neuint.2017.01.007.

Stradomska, T.J., Syczewska, M., Jamroz, E., Pleskaczyńska, A., Kruczek, P., Ciara, E., et al., 2020. Serum very long-chain fatty acids (VLCFA) levels as predictive biomarkers of diseases severity and probability of survival in peroxisomal disorders. PLoS One 15, e0238796. https://doi.org/10.1371/journal.pone.0238796.

Taguchi, Y.V., Liu, J., Ruan, J., Pacheco, J., Zhang, X., Abbasi, J., et al., 2017. Glucosylsphingosine promotes α-Synuclein pathology in mutant GBA-associated Parkinson's disease. J. Neurosci. 37, 9617–9631. https://doi.org/10.1523/JNEUROSCI.1525-17.2017.

Tang, Y., Han, L., Li, S., Hu, T., Xu, Z., Fan, Y., et al., 2023. Plasma GFAP in Parkinson's disease with cognitive impairment and its potential to predict conversion to dementia. NPJ Parkinsons Dis. 9, 23. https://doi.org/10.1038/s41531-023-00447-7.

Tirozzi, A., Modugno, N., Palomba, N.P., Ferese, R., Lombardi, A., Olivola, E., et al., 2021. Analysis of genetic and non-genetic predictors of levodopa induced dyskinesia in Parkinson's disease. Front. Pharmacol. 12. https://doi.org/10.3389/fphar.2021.640603.

Tommasino, C., Marconi, M., Ciarlo, L., Matarrese, P., Malorni, W., 2015. Autophagic flux and autophagosome morphogenesis require the participation of sphingolipids. Apoptosis 20, 645–657. https://doi.org/10.1007/s10495-015-1102-8.

Treede, I., Braun, A., Sparla, R., Kühnel, M., Giese, T., Turner, J.R., et al., 2007. Anti-inflammatory effects of phosphatidylcholine. J. Biol. Chem. 282, 27155–27164. https://doi.org/10.1074/jbc.M704408200.

Wang, J., Wang, F., Mai, D., Qu, S., 2020. Molecular mechanisms of glutamate toxicity in Parkinson's disease. Front. Neurosci. 14. https://doi.org/10.3389/fnins.2020.585584.

Wang, Yuye, Sun, Y., Wang, Yu, Jia, S., Qiao, Y., Zhou, Z., et al., 2023. Urine metabolomics phenotyping and urinary biomarker exploratory in mild cognitive impairment and Alzheimer's disease. Front. Aging Neurosci. 15. https://doi.org/10.3389/fnagi.2023.1273807.

Warensjö, E., Sundström, J., Vessby, B., Cederholm, T., Risérus, U., 2008. Markers of dietary fat quality and fatty acid desaturation as predictors of total and cardiovascular mortality: a population-based prospective study. Am. J. Clin. Nutr. 88, 203–209. https://doi.org/10.1093/ajcn/88.1.203.

Wu, L., Chu, L., Pang, Y., Huo, J., Cao, H., Tian, Q., et al., 2024. Effects of dietary supplements, foods, and dietary patterns in Parkinson's disease: meta-analysis and systematic review of randomized and crossover studies. Eur. J. Clin. Nutr. 78, 365–375. https://doi.org/10.1038/s41430-024-01411-1.

Xicoy, H., Wieringa, B., Martens, G.J.M., 2019. The role of lipids in Parkinson's disease. Cells 8, 27. https://doi.org/10.3390/cells8010027.

Xu, B., Chen, L., Zhan, Y., Marquez, K.N.S., Zhuo, L., Qi, S., et al., 2022. The biological functions and regulatory mechanisms of fatty acid binding protein 5 in various diseases. Front. Cell Dev. Biol. 10. https://doi.org/10.3389/fcell.2022.857919.

Yang, J., Hertz, E., Zhang, X., Leinartaité, L., Lundius, E.G., Li, J., et al., 2016. Overexpression of α-synuclein simultaneously increases glutamate NMDA receptor phosphorylation and reduces glucocerebrosidase activity. Neurosci. Lett. 611, 51–58. https://doi.org/10.1016/j.neulet.2015.11.023.

Yang, Z., Li, T., Li, S., Wei, M., Qi, H., Shen, B., et al., 2019. Altered expression levels of MicroRNA-132 and Nurr1 in peripheral blood of Parkinson's disease: potential

disease biomarkers. ACS Chem. Neurosci. 10, 2243–2249. https://doi.org/10.1021/acschemneuro.8b00460.